AD-A159 822 TRANSMISSION ACOUSTIC VIBRATION TESTING(U) UNITED TECHNOLOGIES CORP STRATFORD CT SIKORSKY AIRCRAFT DIV C YOERKIE ET AL. JUL 85 USAAVRADCOM-TR-83-D-34 1/1

UNCLASSIFIED DAAK51-82-C-0040 F/G 1/3 NL

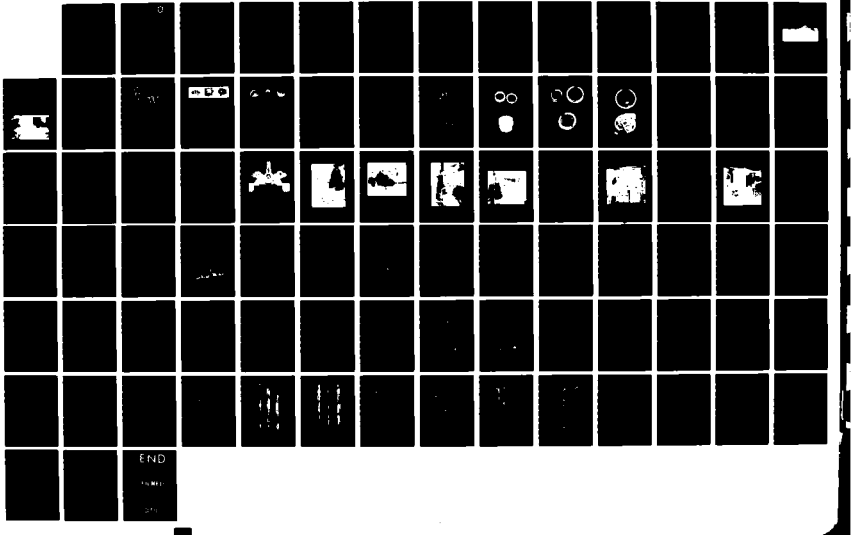

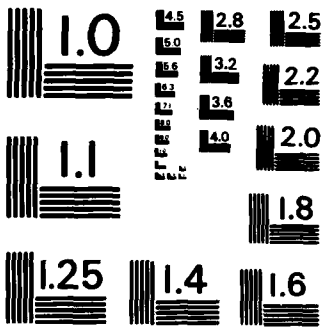

MICROCOPY RESOLUTION TEST CHART
NATIONAL BUREAU OF STANDARDS - 1963 - A

USAAVRADCOM TR-83-D-34

TRANSMISSION ACOUSTIC VIBRATION TESTING

C. Yoerkie, A. Chory

SIKORSKY AIRCRAFT DIVISION
UNITED TECHNOLOGIES CORPORATION
Stratford, Conn. 06602

July 1985

Final Report for Period September 1982 - November 1983

Prepared for

AVIATION APPLIED TECHNOLOGY DIRECTORATE
U.S. ARMY AVIATION RESEARCH AND TECHNOLOGY ACTIVITY (AVSCOM)
Fort Eustis, Va. 23604-5577

AVSCOM — PROVIDING LEADERS THE DECISIVE EDGE

AVIATION APPLIED TECHNOLOGY DIRECTORATE POSITION STATEMENT

This report provides comparative acoustic (high frequency) vibration data on a baseline BLACK HAWK helicopter main transmission and three experimental configurations of that gearbox. Tests were limited because of the existence of only one set of experimental hardware: a stainless steel housing and a high contact ratio planetary gearset. A significant result involving harmonics above the planetary mesh frequency offers a challenge for additional research.

Mr. M. L. Pedersen of the Propulsion Technical Area, Aeronautical Technology Division, served as project engineer for this effort.

Unclassified

SECURITY CLASSIFICATION OF THIS PAGE

REPORT DOCUMENTATION PAGE

1a. REPORT SECURITY CLASSIFICATION Unclassified	1b. RESTRICTIVE MARKINGS
2a. SECURITY CLASSIFICATION AUTHORITY	3. DISTRIBUTION/AVAILABILITY OF REPORT Approved for public release; distribution unlimited.
2b. DECLASSIFICATION/DOWNGRADING SCHEDULE	
4. PERFORMING ORGANIZATION REPORT NUMBER(S)	5. MONITORING ORGANIZATION REPORT NUMBER(S) USAAVRADCOM TR 83-D-34
6a. NAME OF PERFORMING ORGANIZATION Sikorsky Aircraft Division United Technologies Corporation 6b. OFFICE SYMBOL (If applicable)	7a. NAME OF MONITORING ORGANIZATION Aviation Applied Technology Directorate
6c. ADDRESS (City, State and ZIP Code) Stratford, CT 06602	7b. ADDRESS (City, State and ZIP Code) U.S. Army Aviation Research and Technology Activity (AVSCOM) Fort Eustis, Virginia 23604-5577
8a. NAME OF FUNDING/SPONSORING ORGANIZATION 8b. OFFICE SYMBOL (If applicable)	9. PROCUREMENT INSTRUMENT IDENTIFICATION NUMBER
8c. ADDRESS (City, State and ZIP Code)	10. SOURCE OF FUNDING NOS. PROGRAM ELEMENT NO.: 63201A PROJECT NO.: 1L263201D872 TASK NO.: 01 044 WORK UNIT NO.: EK
11. TITLE (Include Security Classification) Transmission Acoustic Vibration Testing	
12. PERSONAL AUTHOR(S) C. Yoerkie, A. Chory	
13a. TYPE OF REPORT Final	13b. TIME COVERED FROM Sep 82 TO Nov 83
14. DATE OF REPORT (Yr., Mo., Day) July 1985	15. PAGE COUNT 75
16. SUPPLEMENTARY NOTATION	

17. COSATI CODES		
FIELD	GROUP	SUB. GR.

18. SUBJECT TERMS (Continue on reverse if necessary and identify by block number)
Helicopter Transmissions; Stainless Steel Housing; High Contact Ratio Gears; Gear Mesh Frequency; Buttress Tooth Gears; Acoustic Vibration

19. ABSTRACT (Continue on reverse if necessary and identify by block number)

Laboratory tests were conducted to determine the individual and combined effects of a high contact ratio (HCR) planetary gearset and a stainless steel housing on the acoustic (high frequency) vibration signature of the BLACK HAWK helicopter main transmission. Vibration levels at the planetary mesh frequency increased significantly with the stainless steel housing, but increased unexpectedly with the HCR planetary. The primary reason for the increased response with the HCR was the reduced gear face widths.

20. DISTRIBUTION/AVAILABILITY OF ABSTRACT UNCLASSIFIED/UNLIMITED ☒ SAME AS RPT. ☐ DTIC USERS ☐	21. ABSTRACT SECURITY CLASSIFICATION Unclassified
22a. NAME OF RESPONSIBLE INDIVIDUAL M. L. Pedersen	22b. TELEPHONE NUMBER (Include Area Code) (804) 878-4105 22c. OFFICE SYMBOL SAVRT-TY-ATP

DD FORM 1473, 83 APR EDITION OF 1 JAN 73 IS OBSOLETE.

Unclassified

SECURITY CLASSIFICATION OF THIS PAGE

PREFACE

This report presents the results of a test program conducted from October 1982 through November 1983 by Sikorsky Aircraft, Division of United Technologies Corporation, under Applied Technology Laboratory Contract DAAK51-82-C-0040.

Technical monitorship for the effort was provided by Mr. M. L. Pedersen of the Applied Technology Laboratory, U.S. Army Research and Technology Laboratories (AVSCOM)* with significant assistance from Mr. J. Coy of the Propulsion Laboratory, U.S. Army Research and Technology Laboratories (AVSCOM) and Mr. F. Oswald of the NASA-Lewis Research Center. Project management was under the direction of Mr. J. Mancini, with Technical direction provided by Messrs. J. Kish and L. Hager. Technical support was provided by Messrs. C. Yoerkie, A. Chory, P. Arcidiacono, R. Schlegel, H. Frint, and R. Haven.

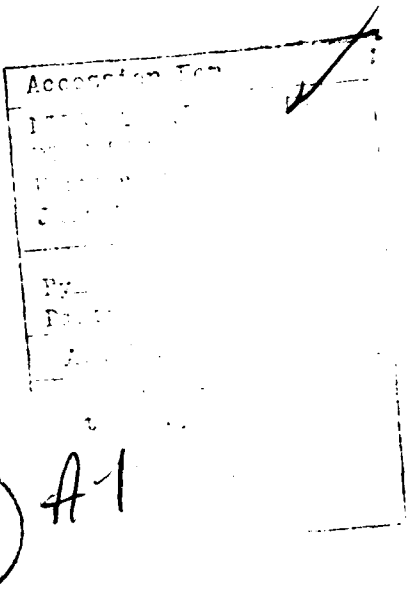

*Redesignated Aviation Applied Technology Directorate, U.S. Army Aviation Research and Technology Activity (AVSCOM), effective 1 July 1985.

TABLE OF CONTENTS

LIST OF ILLUSTRATIONS

LIST OF ILLUSTRATIONS (Continued)

LIST OF ILLUSTRATIONS (Continued)

LIST OF TABLES

INTRODUCTION

Transmission acoustic (high frequency) vibration signatures have become increasingly important because of the weight penalty associated with soundproofing material required to protect the helicopter cabin. As gearboxes have become lighter because of technology advances generally related to structural efficiency, more acoustic treatment has been required because the noise generated by the transmission has increasesd (Figure 1).

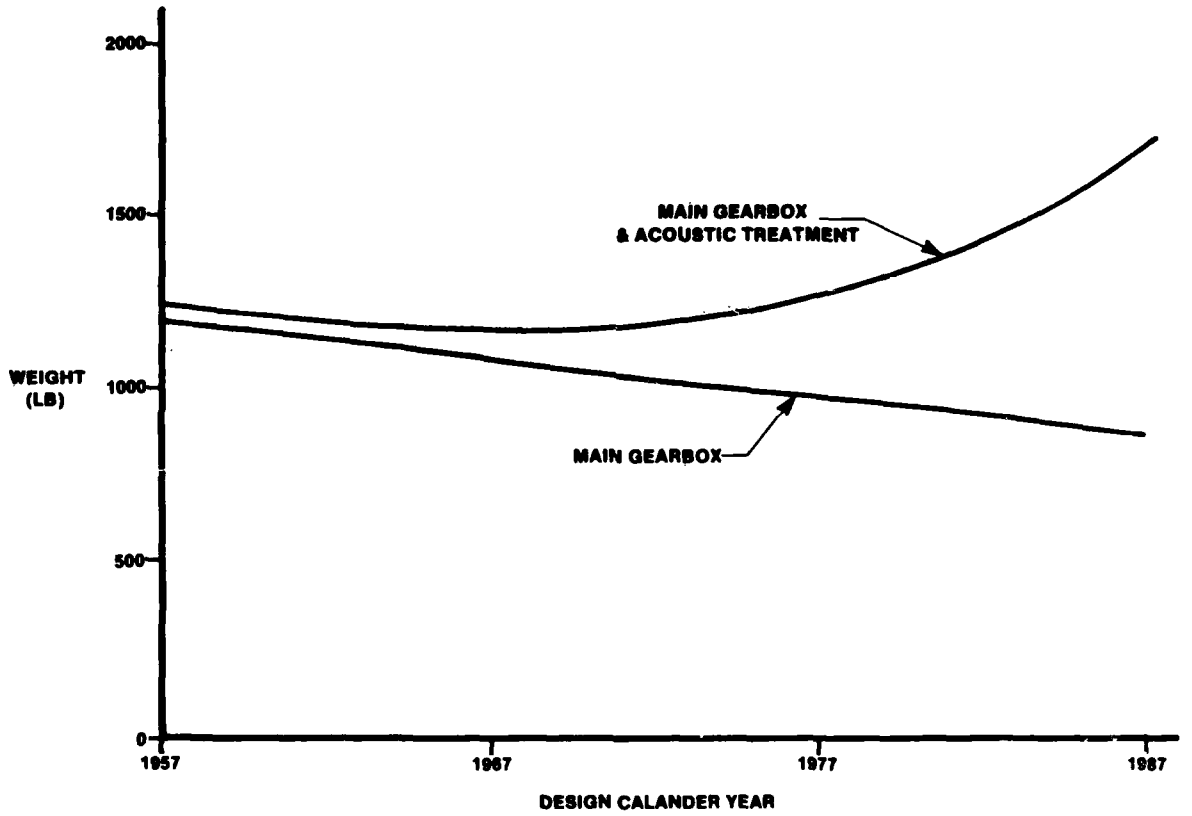

Figure 1. Gearbox and Acoustic Treatment Weight Trends.

The increased noise from lighter weight helicopter transmissions can be attributed to increased gear tooth deflections, higher strain density of the shafting, less energy dissipation, higher vibration inherent in thin-walled housings, and higher dynamic loads transmitted from the transmission to the airframe.

The objective of this program was to assess the effect of two advanced technology components, a stainless steel housing and a high contact ratio planetary gearset, on gearbox vibration in the range of frequencies important to cabin noise. From these comparative vibration signatures, an inference of the effect of these components on cabin noise could be attempted. A more rigorous assessment would require testing several samples of each design on an aircraft to account for statistical variations and for program mounting dynamics; such an evaluation was beyond the scope of this effort.

TEST HARDWARE

GENERAL

The BLACK HAWK helicopter (Figure 2) is the Army's advanced twin-engine utility helicopter manufactured by Sikorsky Aircraft.

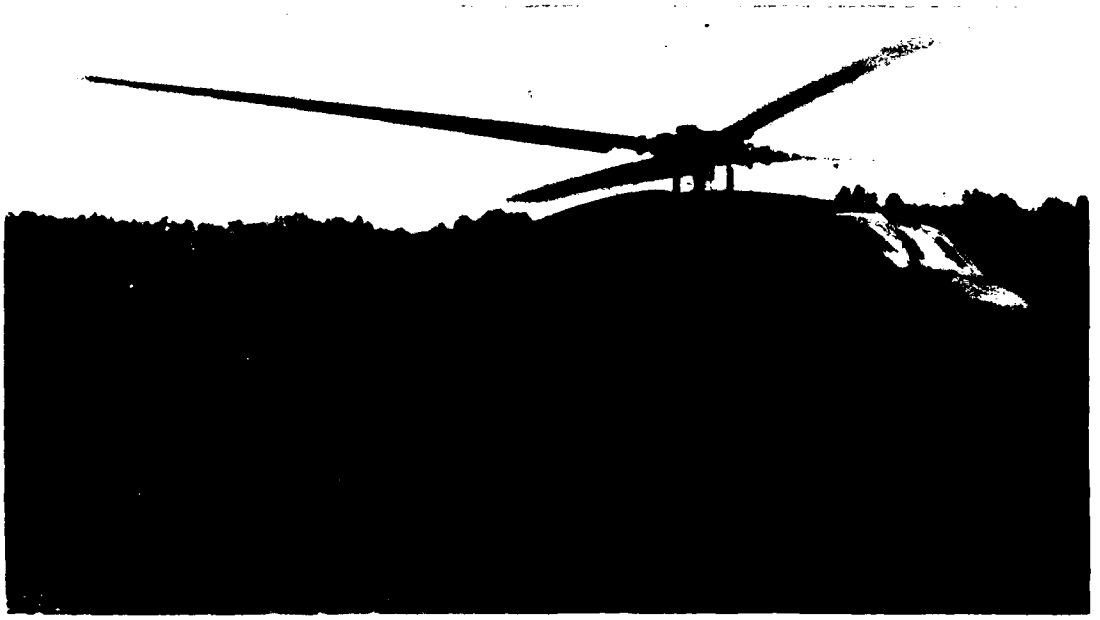

Figure 2. UH-60A BLACK HAWK Helicopter.

Two GE-T700 turboshaft engines deliver power to the BLACK HAWK drive system. The drive system (Figure 3) consists of the main gearbox, which combines engine power, drives the main and tail rotors, and provides secondary subsystem power; the drive shafts, which deliver power to the tail rotor; and the intermediate and tail gearboxes, which provide the proper speed and angle changes for the tail rotor drive system. Rotational speed is reduced from 20,900 rpm at the engines to 258 rpm at the main rotor and 1190 rpm at the tail rotor.

The BLACK HAWK main transmission was used as the baseline in these acoustic vibration tests. This gearbox (Figure 4) weighs 1245 lbs, including the oil cooler and blower and related hardware; the gearbox rating is 2828 SHP. It is of modular construction which permits interchangeability of the left and right input modules and accessory sections.

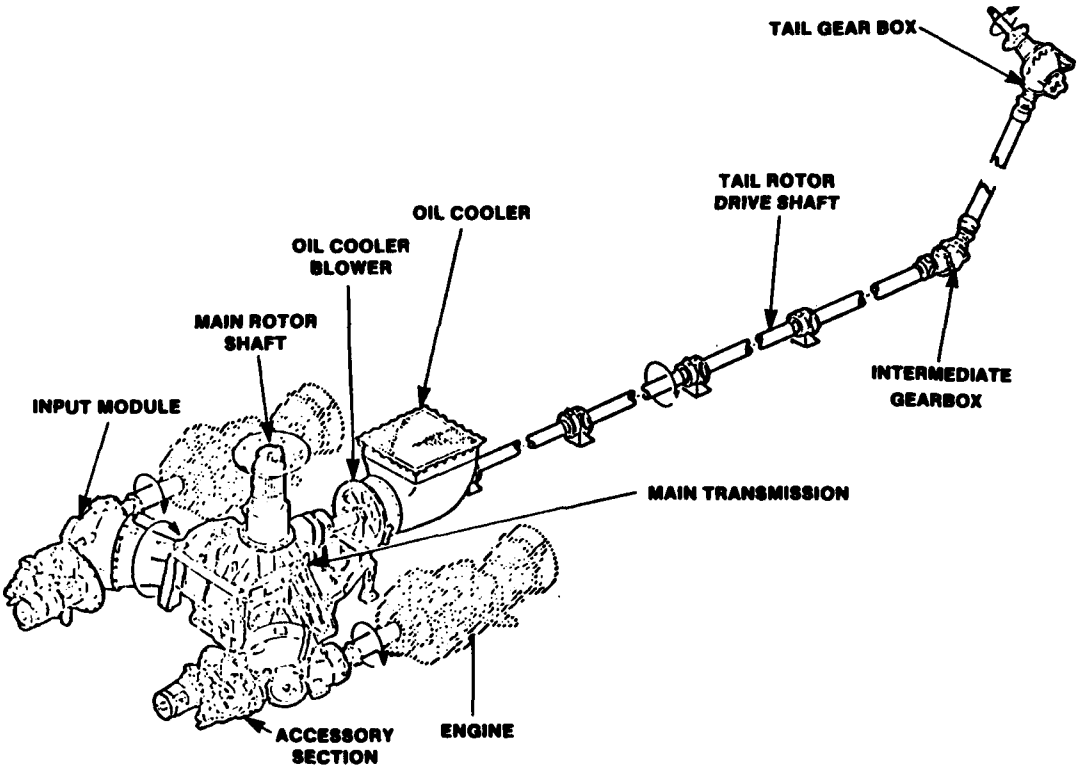

Figure 3. BLACK HAWK Drive System.

Figure 4. BLACK HAWK Main Transmission.

A cross section of the baseline gearbox is shown in Figure 5. Power from two bevel input pinions is combined at the main bevel gear and is transmitted to a single-stage, fixed ring gear planetary unit, the carrier of which is attached to the main rotor shaft; maximum power (takeoff rating) per input module is 1414 SHP.

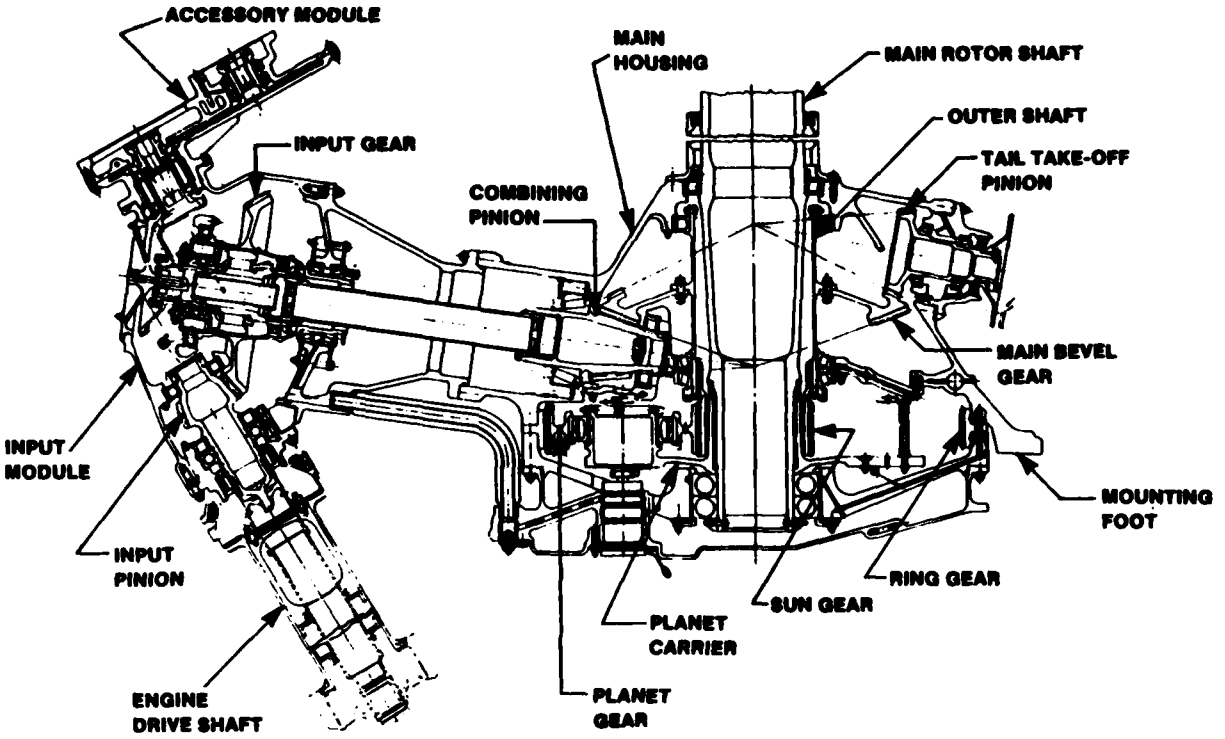

Figure 5. Baseline Gearbox Cross Section.

The ring gear is attached to the main housing near the mounting feet, which attach the transmission to the airframe. Vibrations induced by gearbox internal components and especially by the planetary gearset and the transfer of those vibrations to the airframe cabin impact significantly on internal cabin noise. Since an experimental housing and planetary gearset for the BLACK HAWK transmission were developed under a previous program (Reference 1), these components were appropriate and available for evaluation in this vibration survey. A cross section of the experimental gearbox is shown in Figure 6.

---

1. Advanced Transmission Components Investigation - Steel Housing, Planetary Gearing, and Bearing Development, Sikorsky Aircraft, USAAVRADCOM TR 82-D-11, Applied Technology Laboratory, U.S. Army Research and Technology Laboratories (AVSCOM), Fort Eustis, Virginia (to be published).

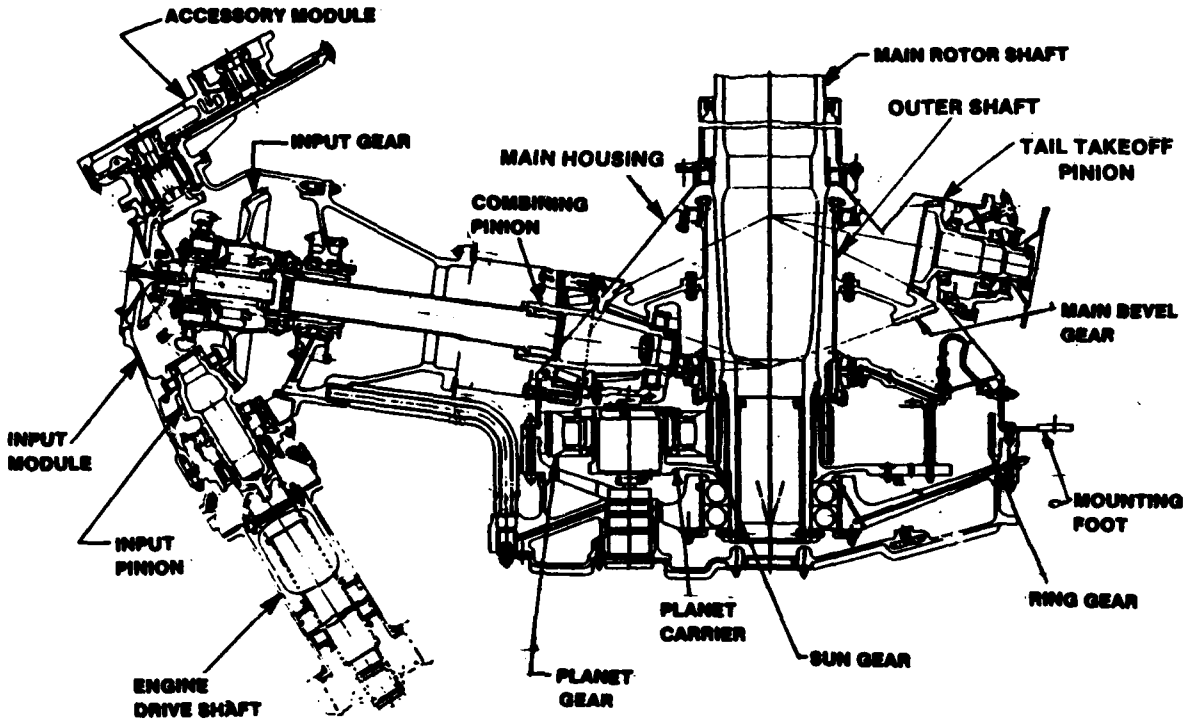

Figure 6. Experimental Gearbox Cross Section.

HOUSING

The baseline housing (Figure 7) is a sand mold ZE41A magnesium alloy casting weighing 153 pounds prior to machining. The housing is then finish machined and weighs 100 pounds. The machined casting is fitted with 444 studs, liners, bushings, and inserts for assembly of the transmission components. The liner and stud assembly weigh 110 pounds. The housing incorporates four mounting feet and mounting rings for two input modules and a tail takeoff assembly. Mounting pads to position the main rotor control brackets are located on the external surface of the housing.

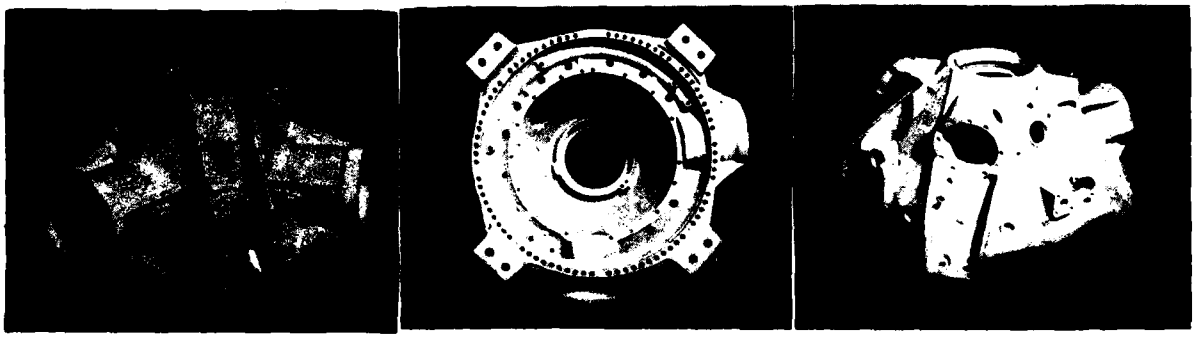

Figure 7. Baseline Magnesium Housing.

A fabricated sheet metal stainless steel main housing was developed as an experimental replacement for the magnesium housing (Reference 1). This housing would be suitable for elevated temperature operation and has good corrosion resistance. The principal design criteria for the fabricated housing were stiffness equal to or greater and weight 20% less than the baseline housing.

The fabricated housing consists of a sheet metal shell with welded stiffening ribs and load bearing struts (Figure 8). The ribs and struts provide the load bearing paths for the input modules and tail takeoff module and transfer rotor loads to the airframe; the shell reacts shear loads and retains the lubricating oil.

The basic structure consists of a frustrum of a cone. The main rotor shaft upper bearing support ring is welded to the top of the cone. A flanged ring is welded at the base of the cone and provides the mounting surface for the planetary ring gear. The flanged ring includes the four mounting feet and the support for the internal straddle mount, which bolts into the fabricated housing and serves as the outer shaft lower bearing support and as the combining pinion bearing supports. The two inputs are cylindrical housings with flanged rings which house the combining pinions and support the input module housings. A cylindrical housing with a flanged ring supports the tail takeoff.

Figure 8. Fabricated Stainless Steel Housing.

PLANETARY GEARSET

In a conventional, standard contact ratio spur gearset the contact ratio falls between one and two (Figure 9). In high contact ratio (HCR) gearing the contact ratio is always greater than two and a minimum of two teeth will be in contact at all times (Figure 10). If the teeth are made with sufficient accuracy, which is the case in most helicopter gears, the high contact ratio gearset has the property of tooth load sharing. Thus, for the same face width, the load per tooth is reduced and the resulting tooth stresses are reduced.

Another approach would be to use the same allowable stresses and thereby reduce the face width and hence gear weight (Reference 1). In combination with the HCR gearing, teeth can be further strengthened by buttressing, where unequal pressure angles exist on the driving and driven sides of the tooth. Figure 11 illustrates an HCR buttress tooth gear having a 20-degree pressure angle on the driving side and a 23-degree pressure angle on the coast side. For the same tooth thickness at the pitch circle, tooth thickness is increased at the base on the coast side, thus reducing tooth bending stresses. With the buttress feature, the advantages of the 20-degree drive side pressure angle are retained; lower pressure angles increase the contact ratio and reduce gear separating loads, presumably leading to smoother, quieter operation.

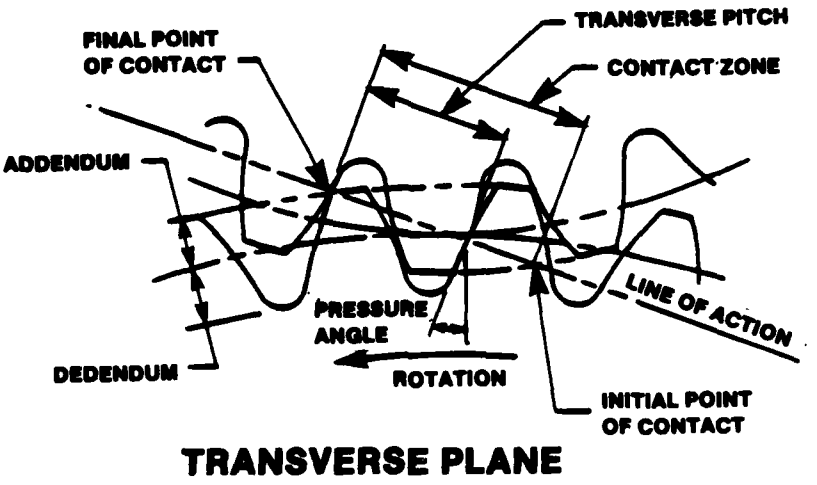

Figure 9. Standard Contract Ratio Gearing.

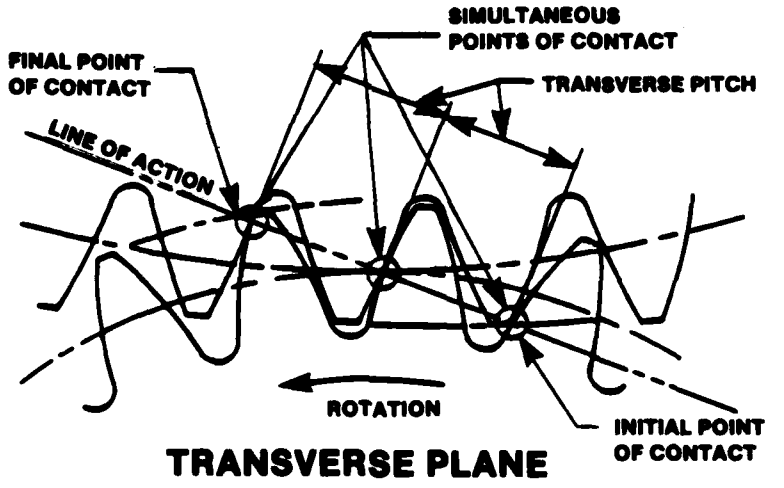

Figure 10. High Contact Ratio Gearing.

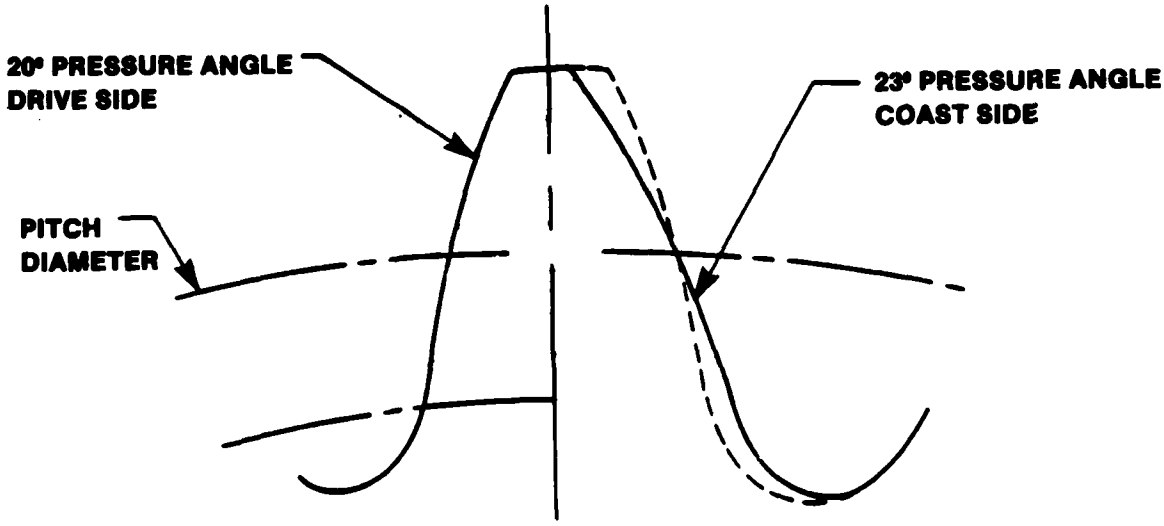

Figure 11. Buttress Tooth Form.

The baseline planetary consists of a cantilevered planet carrier with spherical roller bearings (Figure 12). The planetary receives power from the main bevel gear through a floating spline on the sun gear and transfers it to the main rotor shaft through a locked spline in the carrier.

The experimental HCR buttress planetary (Figure 13) is similar in design to the baseline planetary but has three major differences:

1. Face widths were reduced approximately 15% to save weight by taking advantage of the increased strength of the HCR gear teeth.

2. The spherical roller bearing outer race was integrated with the planet gear.

3. Gear material was changed from AISI 9310 to CBS 600 steel, a high hot hardness gear steel.

HCR buttress components are shown in Figures 14 through 18.

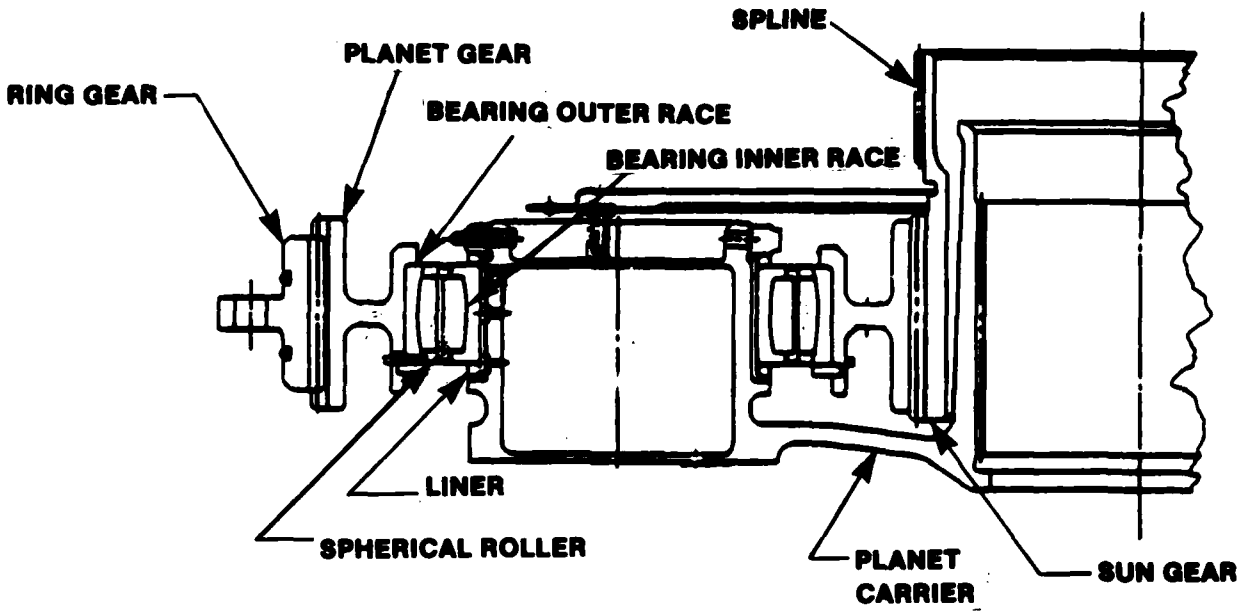

Figure 12. Baseline Planetary.

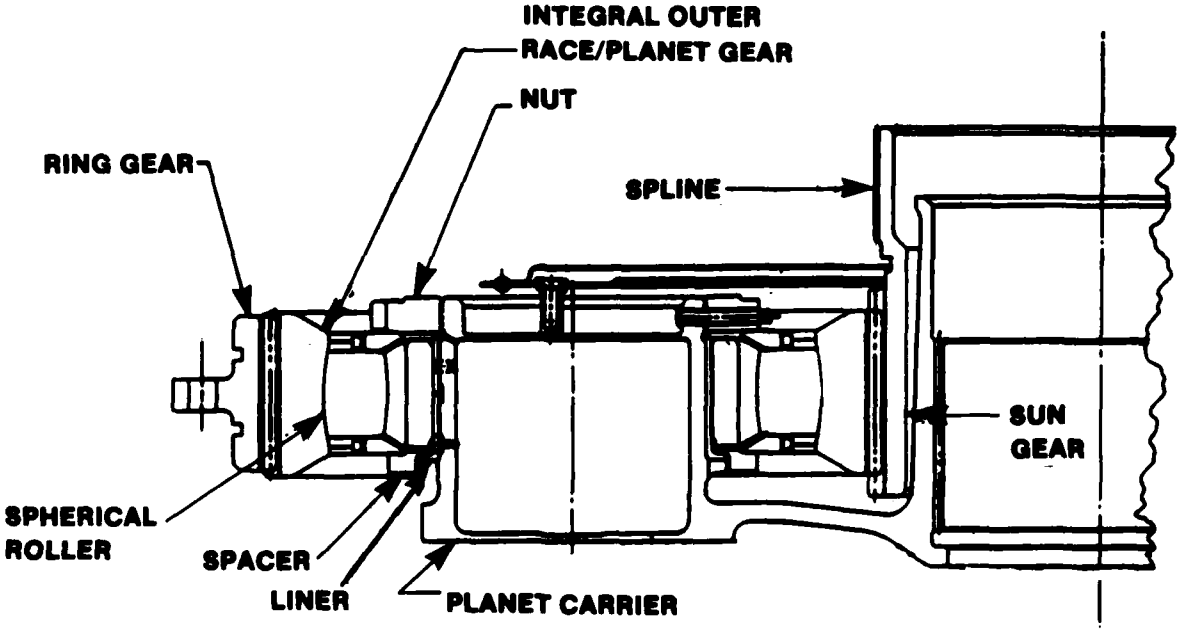

Figure 13. Experimental Planetary.

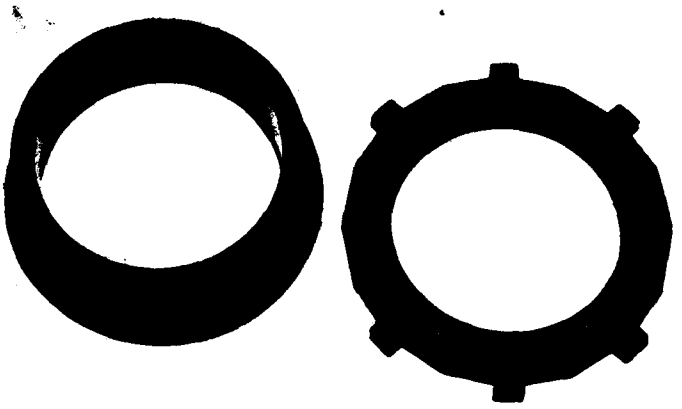

Figure 14. HCR Spacer and Bearing Nut.

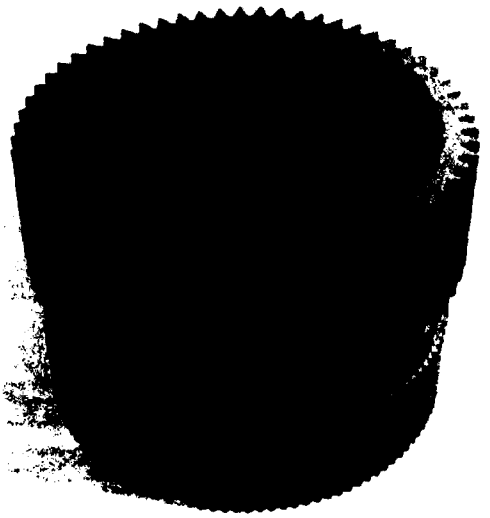

Figure 15. HCR Sun Gear.

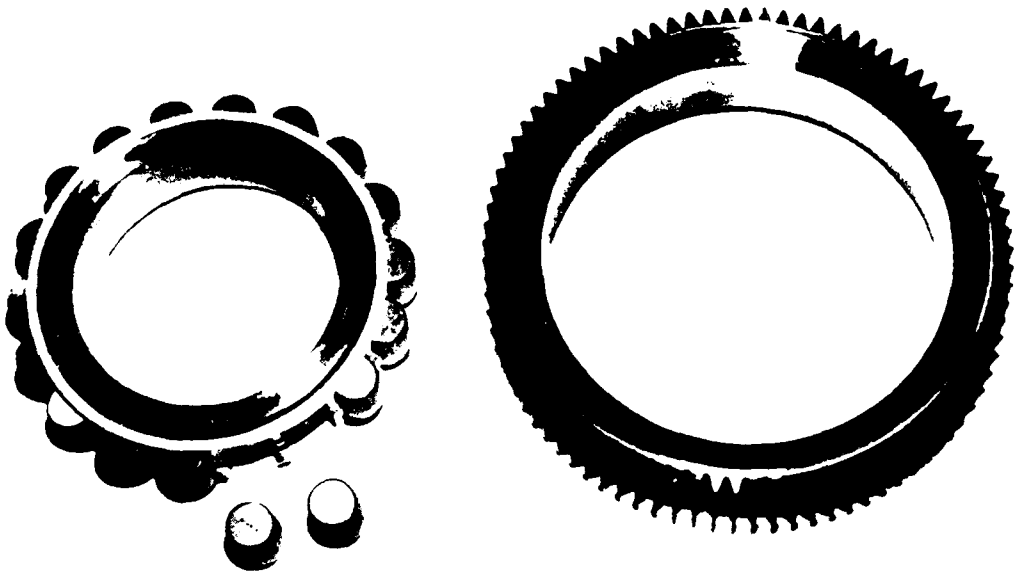

Bearing

Gear

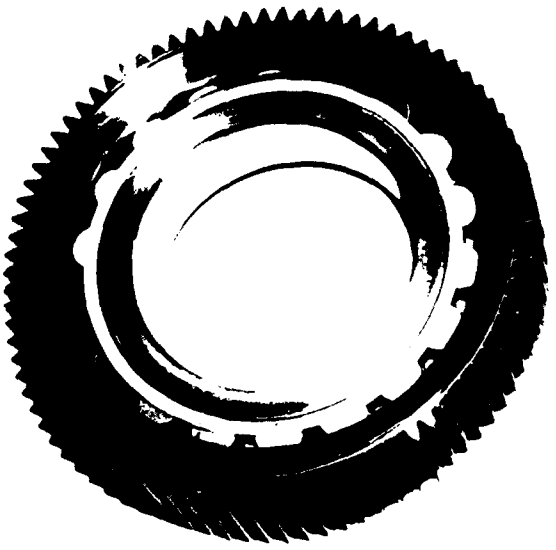

Assembly

Figure 16. HCR Planet Gear/Bearing.

Figure 17. HCR Ring Gear.

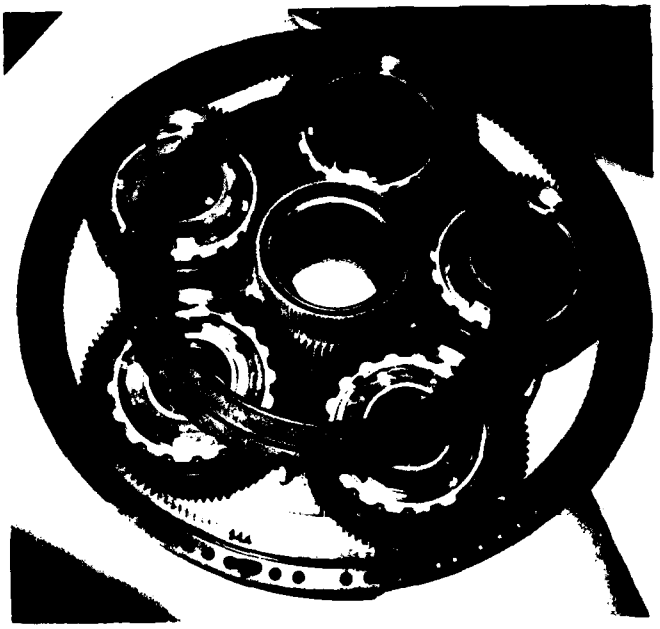

Figure 18. HCR Planetary Assembly.

Part numbers and serial numbers for the planetary gears tested are listed in Table 1. Basic gear tooth data are shown in Tables 2 and 3. Table 2 describes the sun-planet gear mesh data for both configurations. Primary differences in gear tooth geometry are reflected by such key parameters as pressure angle, base circle diameter, and outside diameter. Table 3 lists data for the planet-ring gear mesh.

Table 1. PLANETARY GEARS TESTED

Nomenclature	Part Number	Serial Number
	BASELINE PLANETARY	
Planet Gear 1	70351-08171-105	00063
" " 2	70351-08171-105	00070
" " 3	70351-08171-105	00072
" " 4	70351-08171-105	00073
" " 5	70351-08171-105	00074
Sun Gear	70351-08172-101	B22600020
Ring Gear	70351-08177-101	B22100002
	HCR BUTTRESS PLANETARY	
Planet Gear 1	38017-01102-101	002
" " 2	38017-01102-101	005
" " 3	38017-01102-101	007
" " 4	38017-01102-101	008
" " 5	38017-01102-101	011
Sun Gear	38017-01101-101	011
Ring Gear	38017-01103-101	001

Table 2. SUN-PLANET GEAR MESH DATA

PARAMETER	BASELINE TOOTH FORM		HCR BUTTRESS TOOTH FORM	
	Sun Gear	Planet Gear	Sun Gear	Planet Gear
Number of Teeth	62	83	62	83
Diametral Pitch	8.857	8.857	8.857	8.857
Contact Ratio	1.676	1.676	2.186	2.186
Pressure Angle				
Drive Side	22°30'	22°30'	20°	20°
Coast Side	22°30'	22°30'	23°	23°
Pitch Diameter (in)	7.000	9.3711	7.000	9.3711
Base Circle Diameter (in)				
Drive Side	6.4673	8.6578	6.5780	8.8060
Coast Side	6.4673	8.6578	.4436	8.6262
Outside Diameter (in)	7.2259/ 7.2209	9.5970/ 9.5920	7.3756/ 7.3706	9.5970/ 9.5920
Root Diameter (in)	6.7324/ 6.7224	9.0888 9.0788	6.7291/ 6.7191	8.9505 8.9405
Chordal Tooth Thickness (in)	.1758/ .1748	.1758/ .1748	.1940/ .1930	.1577/ .1567
Chordal Addendum (in)	.1140/ .1115	.1137/ .1112	.1877/ .1852	.1129/ .1104
Index Variation (in)	.0008	.0008	.0008	.0008
Spacing Variation (in)	.0002	.0002	.0002	.0002
Maximum True Involute Form Diameter (in)	6.8073	9.1563	6.8289	9.1033/ 9.0480
Rotational Backlash (in)	.003/ .005	.003/ .005	.005/ .003	.005/ .003
Minimum Fillet Radius (in)	.055	.047	.032	.025
Face Width (in)	3.200	2.970	2.300	2.540

Table 3. PLANET-RING GEAR MESH DATA

PARAMETER	BASELINE TOOTH FORM		HCR BUTTRESS TOOTH FORM	
	Planet Gear	Ring Gear	Planet Gear	Ring Gear
Number of Teeth	83	228	83	228
Diametral Pitch	8.857	8.857	8.857	8.857
Contact Ratio	1.771	1.771	2.189	2.189
Pressure Angle				
Drive Side	22°30'	22°30'	20°	23°
Coast Side	22°30'	22°30'	23°	20°
Pitch Diameter (in)	9.3711	25.7424	9.3711	25.7424
Base Circle Dia. (in)				
Drive Side	8.6578	23.7828	8.8060	23.6960
Coast Side	8.6578	23.7828	8.6262	24.1899
Outside (Inside on Ring) Dia.(in)	9.5970/ 9.5920	25.5215/ 25.5165	9.5970/ 9.5920	25.3781/ 25.3731
Root Diameter (in)	9.0888/ 9.0788	26.0368/ 26.0268	8.9505/ 8.9405	26.0234/ 26.0134
Chordal Tooth Thickness (in)	.1758/ .1748	.1758/ .1748	.1577/ .1567	.1940/ .1930
Chordal Addendum (in)	.1137/ .1112	.1151/ .1126	.1129/ .1104	.1846/ .1821
Index Variation (in)	.0008	.0012	.0008	.0008
Spacing Variation (in)	.0002	.0003	.0002	.0002
Maximum True Involute Form (in)	9.1563	25.9596	9.1033/ 9.0480	25.9413
Rotational Backlash	.005/ .003	.005/ .003	.005/ .003	.005/ .003
Minimum Fillet Radius (in)	.047	.048	.025	.025
Face Width (in)	2.970	2.380	2.540	2.000

TEST CONFIGURATIONS

In addition to the stainless steel housing and HCR planetary gearset, a thrust-carrying cylindrical roller bearing was developed as an experimental replacement for the conventional ball-roller bearing combination on the high speed input pinions in the BLACK HAWK transmission (Reference 1). These roller bearings were used in the input modules of the four primary gearbox configurations tested during this program (the production gearbox retained conventional ball-roller combinations), essentially to accrue additional running time; they were not involved in this program and did not affect the results.

The following configurations were tested:

- Baseline transmission (with input roller bearings).
- Baseline transmission with the HCR planetary (and input roller bearings).
- Baseline transmission with the stainless steel housing (and input roller bearings).
- Baseline transmission with the stainless steel housing and the HCR planetary (and input roller bearings).
- Production transmission (production BLACK HAWK).

INSTRUMENTATION

The range of frequencies of vibration levels which potentially contribute to the acoustic characteristics of an aircraft is approximately 400 to 6000 Hz. The instrumentation system (Figure 19) included accelerometers (B&K Model 4321 triaxials at the foot locations and B&K Model 4375 elsewhere), charge amplifiers (B&K Model 2635), tape recorder, analyzer (HP 5423A), and plotter appropriate for these relatively high frequency vibration measurements. Eighteen accelerometers were installed on the main and input module housings. Details of locations and the transmission components contributing the primary vibration signature are listed in Table 4. Figure 20 shows the accelerometer scheme for the baseline gearbox. An overall view of the test transmission with the stainless steel housing is shown in Figure 21. Detailed views of several accelerometers are shown in Figures 22 through 25 (numbers are keyed to Table 4). The production BLACK HAWK main gearbox was tested with only limited instrumentation (two accelerometers on the ring gear, one on the tail takeoff ring, and one on the left input ring).

Prior to testing each configuration, all instrumentation and wiring were checked and calibrated. Calibration signals were recorded on tape. The tape recorder was run at 30 inches per second in the wide band mode to achieve optimum frequency response while maintaining low phase distortion characteristics; one channel was reserved for voice annotation of the test conditions, while another channel recorded a time code signal to facilitate subsequent data reduction. After each gearbox reached a steady-state operating condition, the conditioned accelerometer signals were recorded for approximately 2 minutes. This provided sufficient data for the analyzer to produce 64 individual fast Fourier transforms for each test condition; these 64 spectra were averaged to form each of the composite amplitude spectra shown in this report. The analyzer was operated on auto spectrum and free run trigger.

Table 4. ACCELEROMETER IDENTIFICATION

Number	Location	Component	Direction
	Main Housing		
1	Forward Foot	Attachment Point	Longitudinal
2	Forward Foot	Attachment Point	Lateral
3	Forward Foot	Attachment Point	Vertical
4	Left Foot	Attachment Point	Longitudinal
5	Left Foot	Attachment Point	Lateral
6	Left Foot	Attachment Point	Vertical
7	Tail Takeoff Ring	Tail Takeoff Bearing	Vert/Radial
8	Upper Right Rib	Outer Shaft Upper Bearing	Longitudinal
9	Upper Right Rib	Outer Shaft Upper Bearing	Lat/Radial
10	Upper Right Rib	Outer Shaft Upper Bearing	Vertical
11	Left Input Ring	Combining Pinion Bearing	Vert/Radial
12	Right Input Ring	Combining Pinion Bearing	Vert/Radial
13	Lower Flange	Ring Gear	Lat/Radial
14	Center Cone	Housing Sidewall	Normal
	Input Module Housings		
15	Left Inner	Input Gear Bearings	Vert/Radial
16	Left Outer	Input Pinion Bearings	Lat/Radial
17	Right Inner	Input Gear Bearings	Vert/Radial
18	Right Outer	Input Pinion Bearings	Lat/Radial

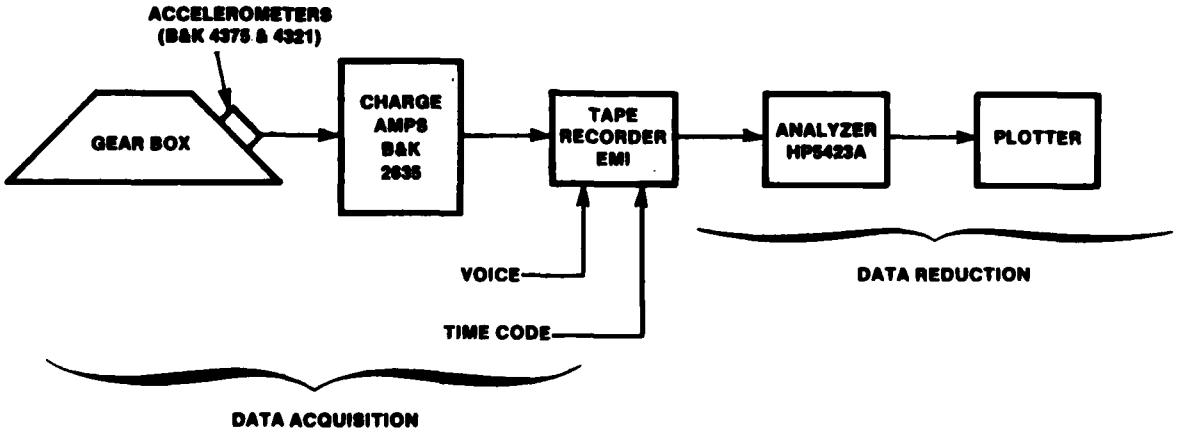

Figure 19. Instrumentation System.

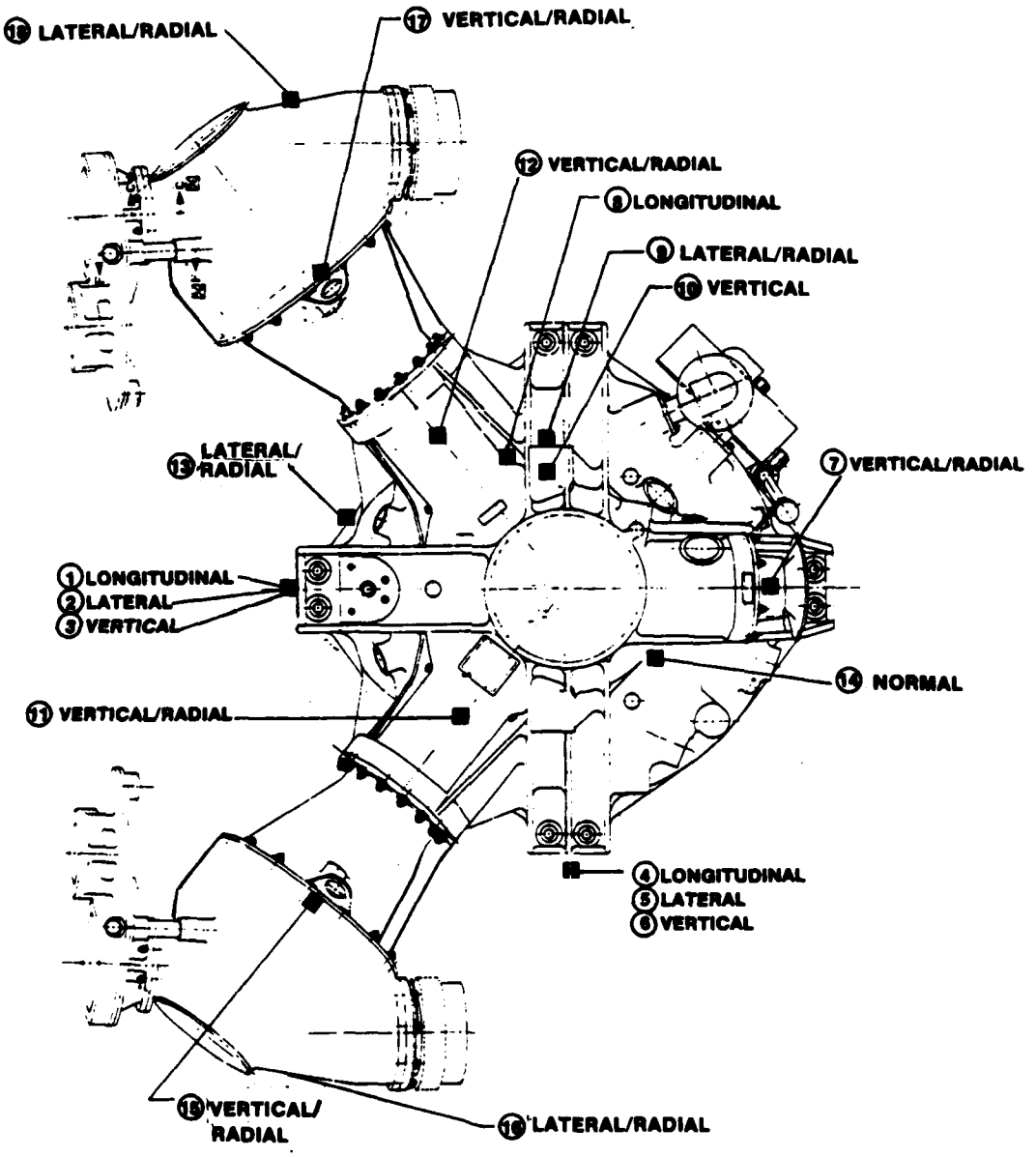

Figure 20. Baseline Gearbox Accelerometer Scheme.

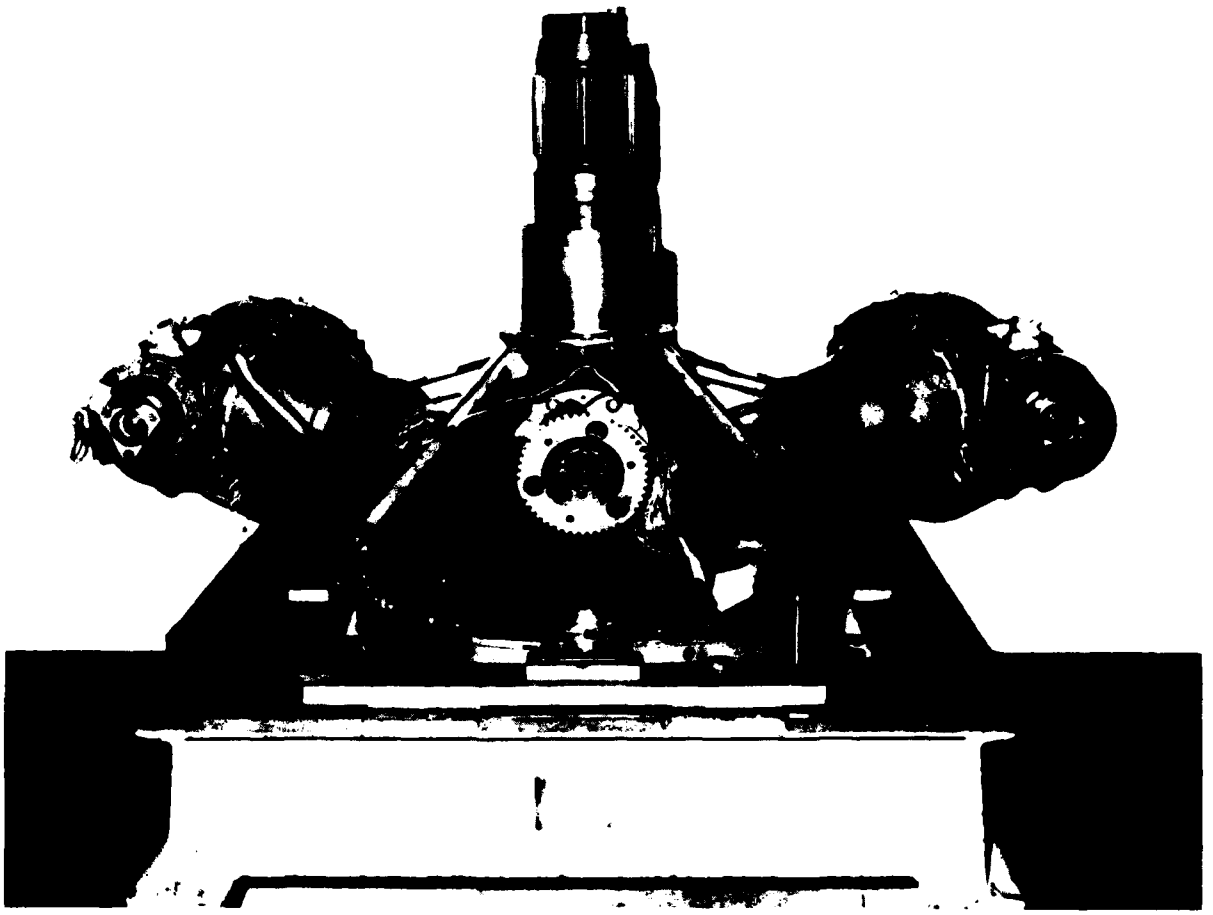

Figure 21. Instrumented Transmission Overall View.

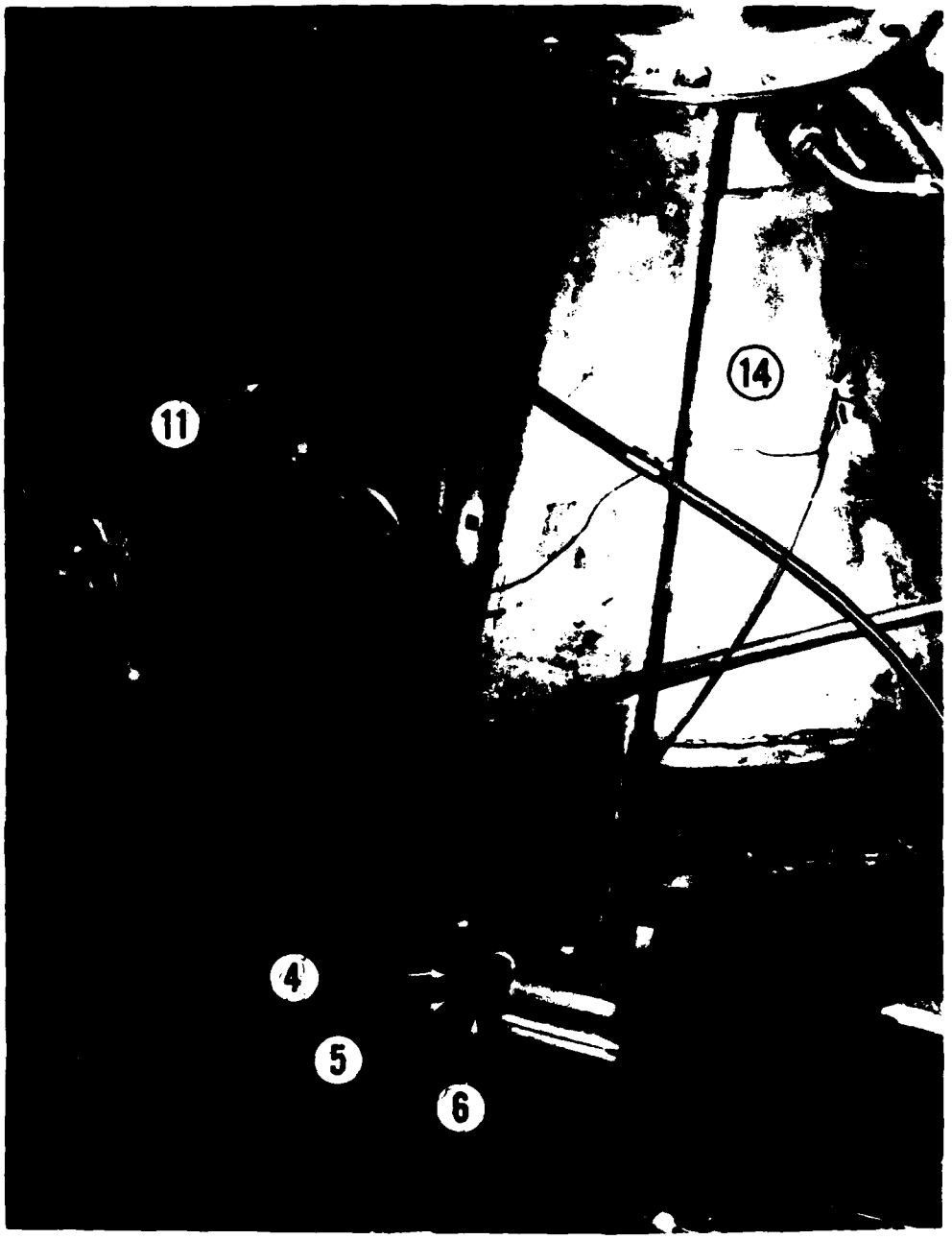

Figure 22. Accelerometers on Left Foot.

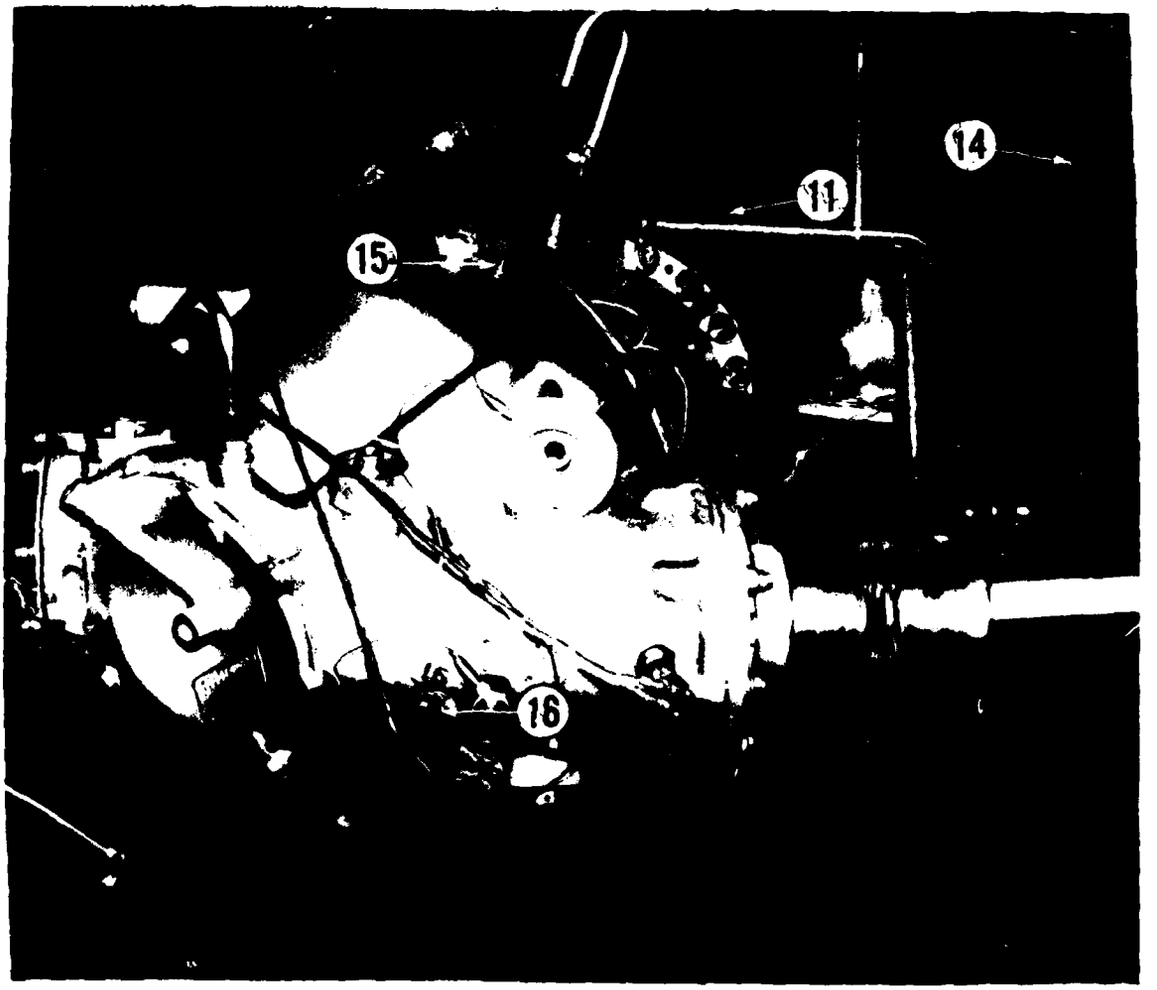

Figure 23. Accelerometers on Left Side.

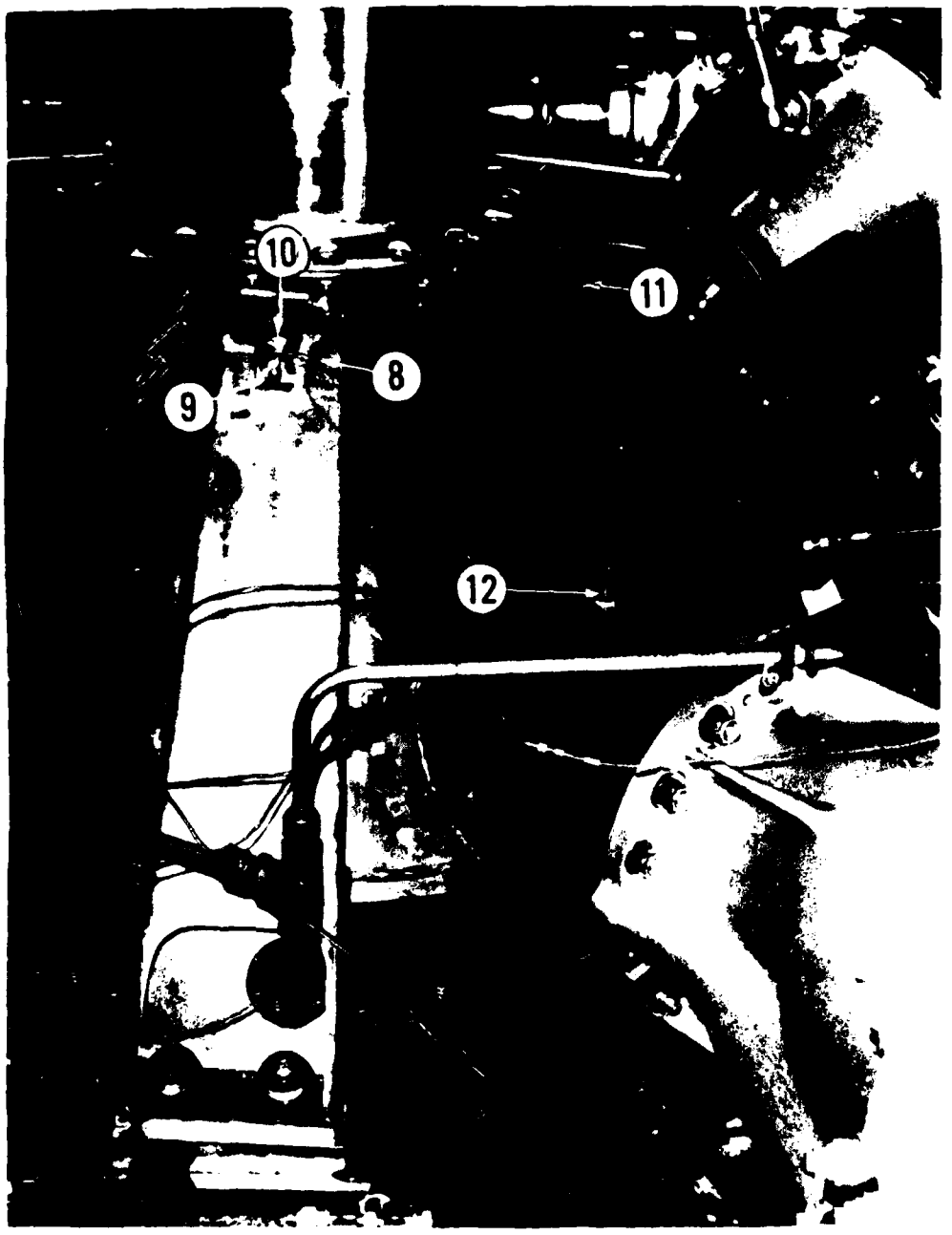

Figure 24. Accelerometers on Right Side.

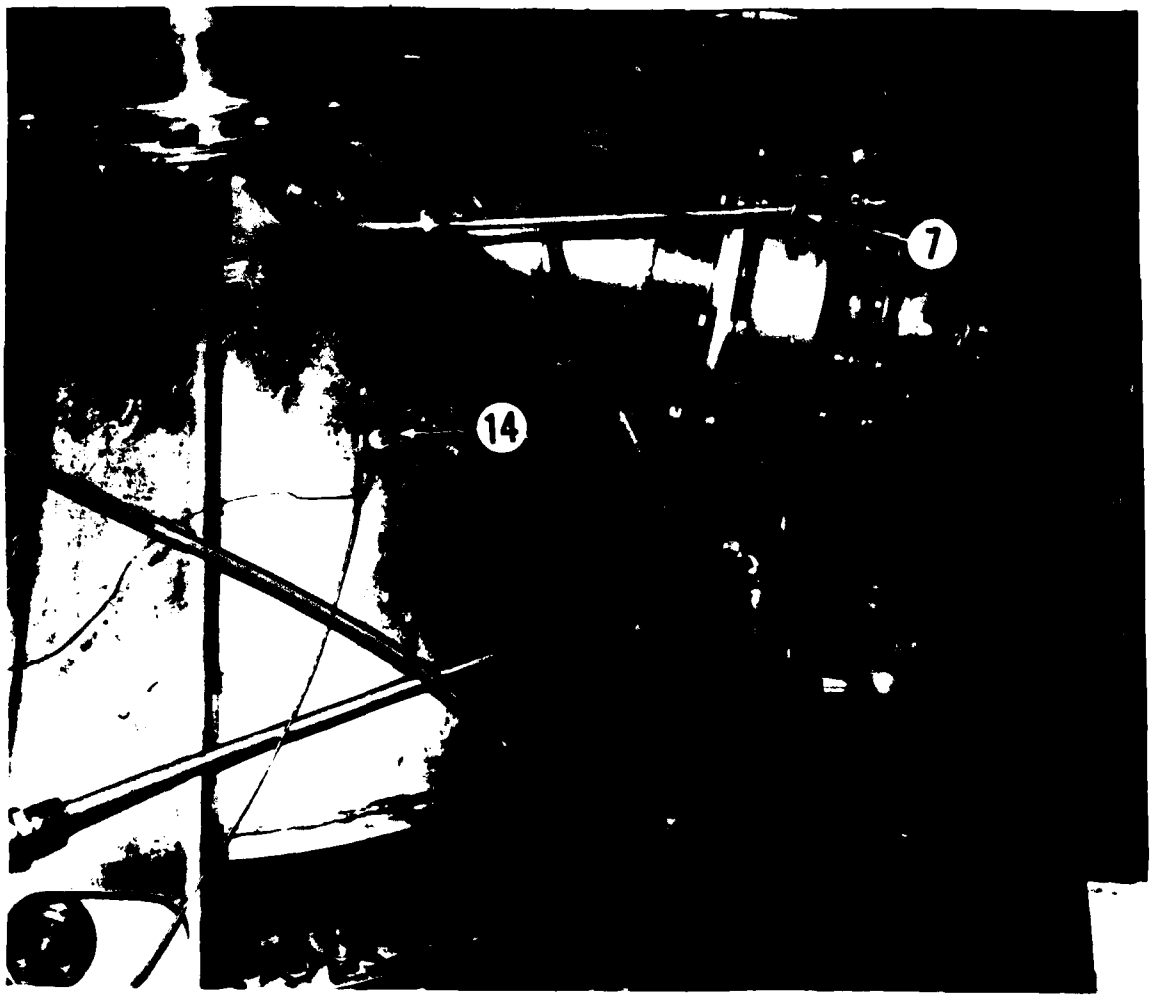

Figure 25. Accelerometers on Rear.

TEST FACILITY

All testing was conducted in the BLACK HAWK main transmission test facility (Figure 26). This facility was designed for full load, full speed testing of production BLACK HAWK gearboxes and employs a regenerative torque principle. The test gearbox, six commercial gearboxes, and a slave gearbox form one or more closed mechanical loops (Figure 27). Each closed loop can be dynamically torqued to produce representative gear and bearing loads in the test gearbox. Loading is achieved with helical gear type torquing devices which can be activated while rotating, thus avoiding start up under load. This regenerative setup uses approximately 10 percent of the power of a load absorber system because the drive motors supply power only to overcome frictional losses. The slave gearbox is a production gearbox modified to operate in reverse and is used to simplify the torque loops.

The control and instrumentation consoles (Figure 28) were adjacent to the test facility in a protected area. Although all key parameters were monitored with measuring devices, a window directly behind the console allowed the operator to observe oil leakage or other gross fault indications. The primary control inputs of speed and load were directly in front of the operator. Dual functioning pressure and temperature gages are shown on the far right, above which are warning indicators such as chip detectors or rapid pressure change warning lights. The buttons between the primary controls and gages are the motor start-up switches. Directly to the left are the oil flow and vibration meters, used to detect low frequency vibration-induced distress in the test or facility gearboxes. On the far left are the data recording devices and automatic shutoff switches. The facility was completely controlled from this console; instrumentation for recording acoustic vibration measurements was an independent system which could be interfaced with the main facility when desired.

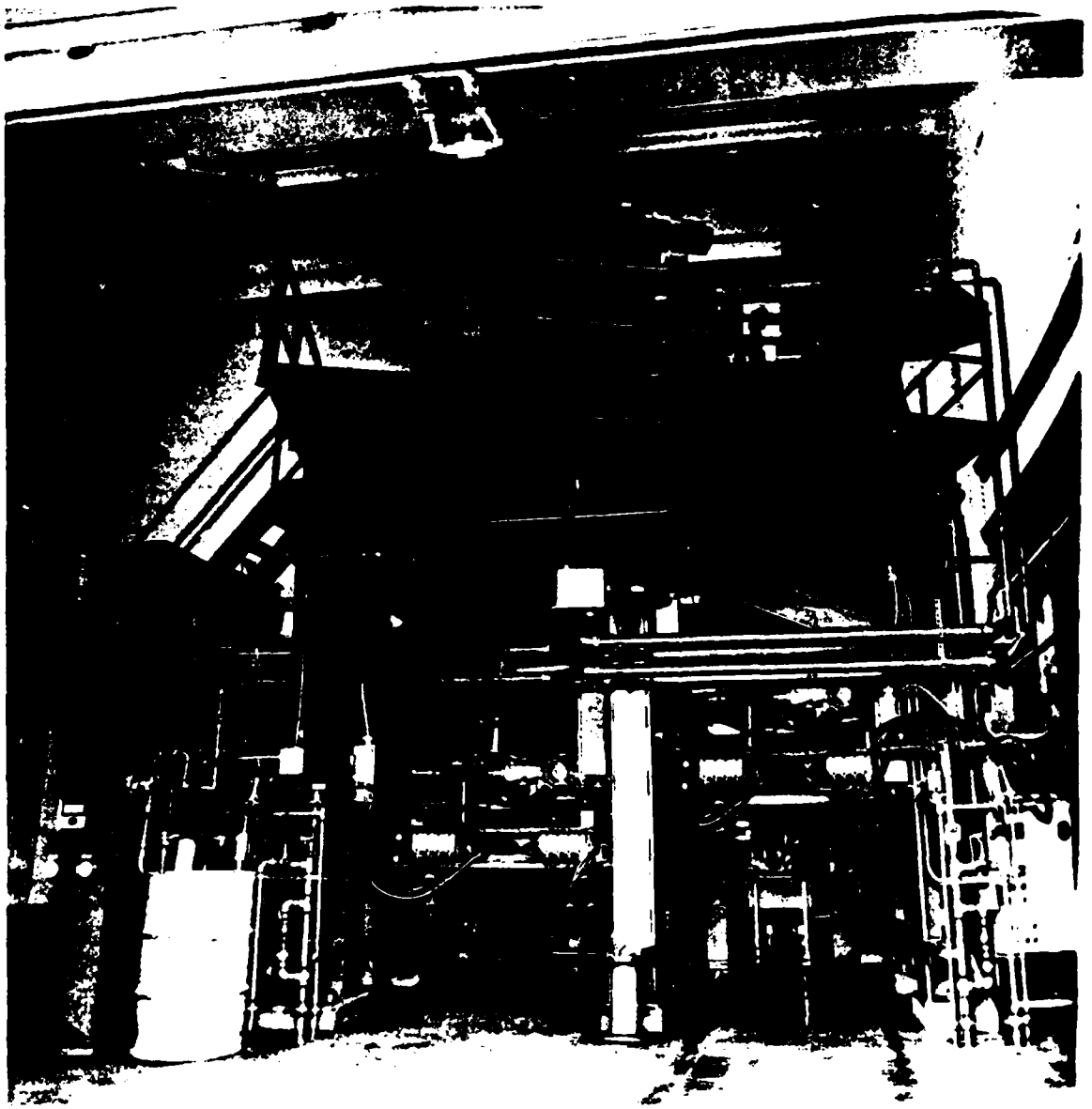

Figure 26. Transmission Test Facility.

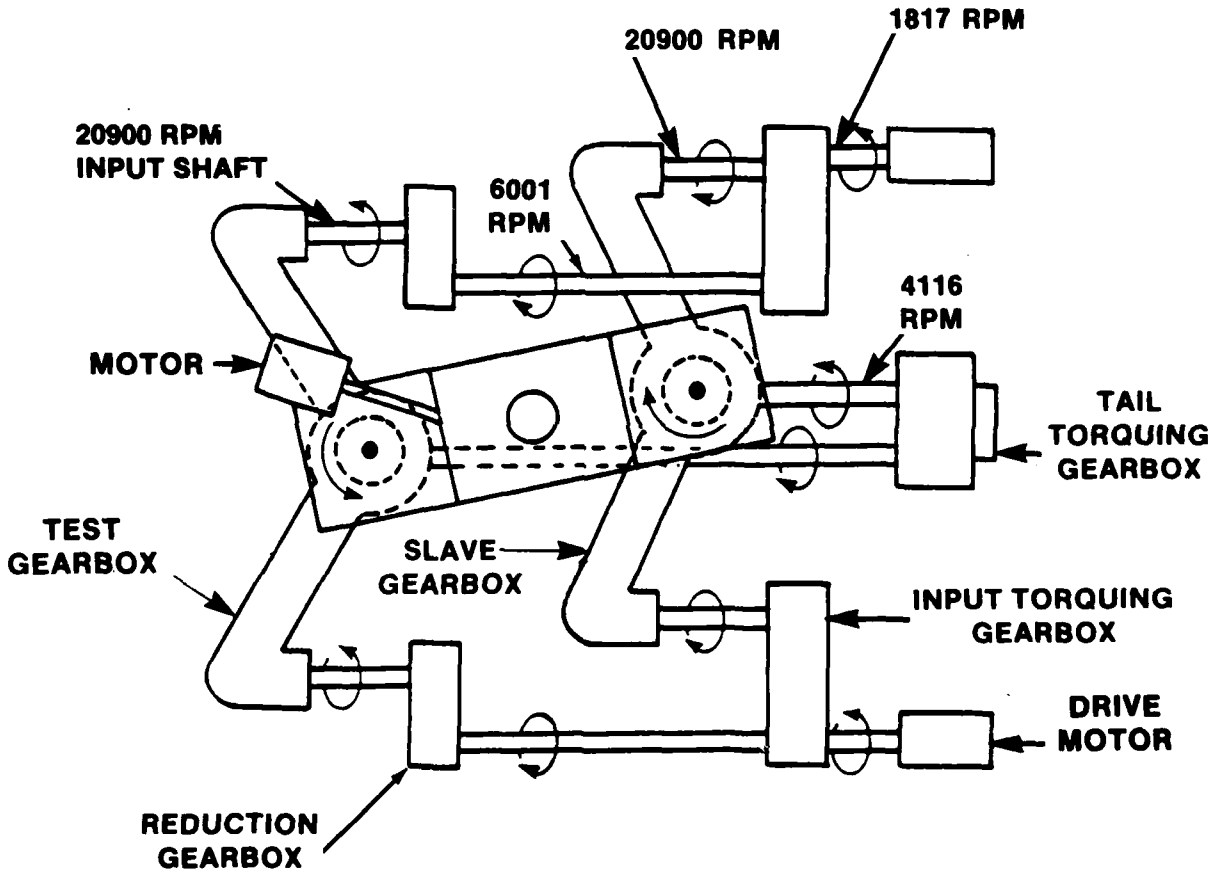

Figure 27. Test Facility Schematic.

Figure 28. Test Facility Console.

PROCEDURE

Each test gearbox configuration was assembled and installed in the test stand and then fully instrumentated and serviced.

After satisfactory check of all instrumentation at low speed and load levels, speed was increased to 100 percent normal operating speed and inlet lube oil stabilized at 160 ± 4°F. Testing was then conducted as specified in Table 5.

Table 5. TEST SEQUENCE

Test Condition	Power (SHP) Left Input	Right Input	Tail Takeoff	Percent Speed
1	500	500	100	100
2	750	750	100	100
3	1000	1000	100	100
4	1000	1000	200	100
5	1250	1250	200	100
6	1400	1400	200	100
7	1000	1000	100	96
8	1000	1000	100	98
9	1000	1000	100	100
10	1000	1000	100	102
11	1000	1000	100	104
12	1000	1000	100	106
13	1000	1000	100	108
14	1000	1000	100	110

Power and speed were varied independently, and each test condition was maintained for a sufficient length of time to normalize gearbox operating parameters and record the required test data. After the variable load testing, speed was varied in incremental steps of 2 percent (variations in helicopter rotor speed can result from fluctuations in engine speed or from an overspeed condition during autorotation). Data were acquired on the production gearbox at three locations (with two accelerometers on the lower flange to insure taking data at the critical ring gear location) for a few speeds and torques because measurements were limited to a four-channel tape recorder during this test.

RESULTS AND ANALYSIS

CABIN NOISE AND ACOUSTIC VIBRATION

The objective of this test was to assess the effect on vibratory excitation levels (which impact cabin acoustic levels) of the two experimental gearbox components. Therefore, it was important to identify the sources of BLACK HAWK cabin noise and the frequencies at which they are generated. Acoustic measurements were taken in the BLACK HAWK cabin with a microphone and tape recorder. These measurements and the related analysis were conducted under a separate program (Reference 2).

The tape recordings were analyzed using fast Fourier transforms to identify those frequencies at which cabin noise levels were generated. The noise level or sound pressure level is described as

$$L_p = 20 \log (P/P_o) \qquad (1)$$

where L_p = sound pressure level in dB

P = pressure measured with sound level meter

P_o = reference pressure = 20μ Pascal = $(20 \times 10^{-6}$ Pascal) x (1 psi/6.895×10^{3} Pascal) = 2.901×10^{-9} psi

Figure 29 is a narrow band sound pressure level spectrum at the center of the BLACK HAWK cabin with the helicopter cruising at 150 kt; transmission gear mesh frequencies are labeled. The absolute decibel levels are not shown because acoustic narrow band noise data are classified. Although the nominal audible range of frequencies is approximately 20 to 18,000 Hz, the critical hearing range is 500 to 5000 Hz in terms of both annoyance and speech interference; the planetary mesh and its second through fifth harmonics are clearly dominant in this important frequency range. A major path of vibratory energy at this mesh frequency appears to be from the ring gear, through the housing to the attachment points, and into the airframe. This vibratory energy, once in the airframe, radiates from panels and windows into the cabin in the form of acoustic energy or noise. Consequently, ring gear accelerometer vibration levels at acoustic frequencies provide an appropriate indicator for comparing the effect of various gearbox modifications on cabin noise levels.

---

2. Data from Contract No. DAAJ01-73-C-0006, Flight Vehicle Internal Noise Survey For The UH-60A.

For conventional gearing the mesh frequency is defined as

$$\text{Mesh Frequency} = (\text{RPM}/60)\ X\ (\text{number of teeth}) \quad (2)$$

For a simple planetary (rotating input sun gear, fixed ring gear, and rotating planetary carrier for the output as in the BLACK HAWK), the planetary gear mesh frequency, f_{pm}, is

$$f_{pm} = (N_s/60)(1-S/(S + R))\ S \quad (3)$$

where (from Tables 2, 3, and 6)

S = 62 teeth = No. of teeth on sun gear

R = 228 teeth = No. of teeth on ring gear

N_s = 1206.3 RPM = sun gear speed

therefore,

$$f_{pm} = (1206.3/60)(1-62/(62+228))X62 = 980\ \text{Hz} \quad (4)$$

Table 6. BLACK HAWK MAIN GEARBOX FREQUENCIES

Source (at 100% Speed)	Rotational Speed (RPM)	Rotational Speed (Hz)	Gear Teeth	Mesh (Hz)
Input Pinion	5747.5	95.8	17	1628.5
Main Bevel Gear	1206.3	20.1	81	1628.5
Sun Gear	1206.3	20.1	62	1246.5
Planet Gear (about its axis)	450.5	7.5	-	-
Planet Gear	708.4	11.8	83	980.0
Ring Gear	-	-	228	-
Tail Takeoff	4115.5	68.6	34	2332.1
Lube Pump	3266.6	54.4	12	653.3
Output Shaft	257.9	4.3	-	-

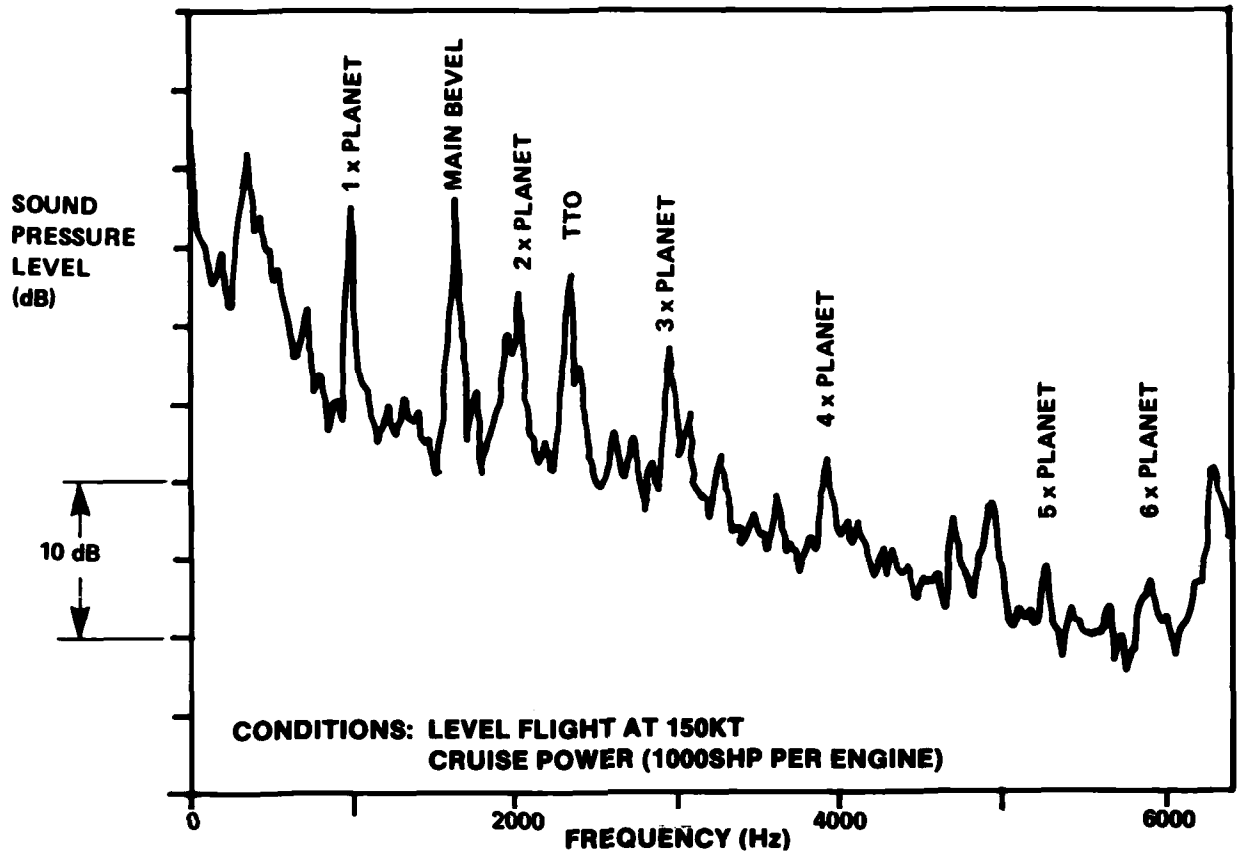

Figure 29. BLACK HAWK Cabin Sound Pressure Levels.

Test results associated with acoustic vibration measurements are extensive because of the number of accelerometers, the variability in speed and power, and the wide range of excitation frequencies. A relative logarithmic scale was used, which gives vibration levels in decibels (dB). For a measured acceleration the vibration or acceleration level is

$$L_a = 20 \log_{10} \left(\frac{a}{a_{ref}}\right) \qquad (5)$$

where L_a = acceleration level (dB)

a = measured acceleration, in/sec^2

a_{ref} = reference acceleration = 1 micro g

= (1 x 10^{-6}g) x (386 in/sec^2 per g)

= 3.86 x 10^{-4} in/sec^2

g = gravitational acceleration = 386 in/sec^2

A power spectral density (PSD) plot of the baseline gearbox vibration from the accelerometer mounted on the ring gear is shown in Figure 30. Since the value of the peak vibration is approximately 129 dB, the measured acceleration is

$$a = 10^{(L_a/20)} \times a_{ref} = 10^{6.45} \times 3.86 \times 10^{-4} \qquad (6)$$

$$a = 1090 \text{ in/sec}^2 = 2.82g$$

Using a reference acceleration shows how accelerometer measurements can be converted to PSD plots; the actual PSD reference is given as $10^{-6}\ g^2/Hz$.

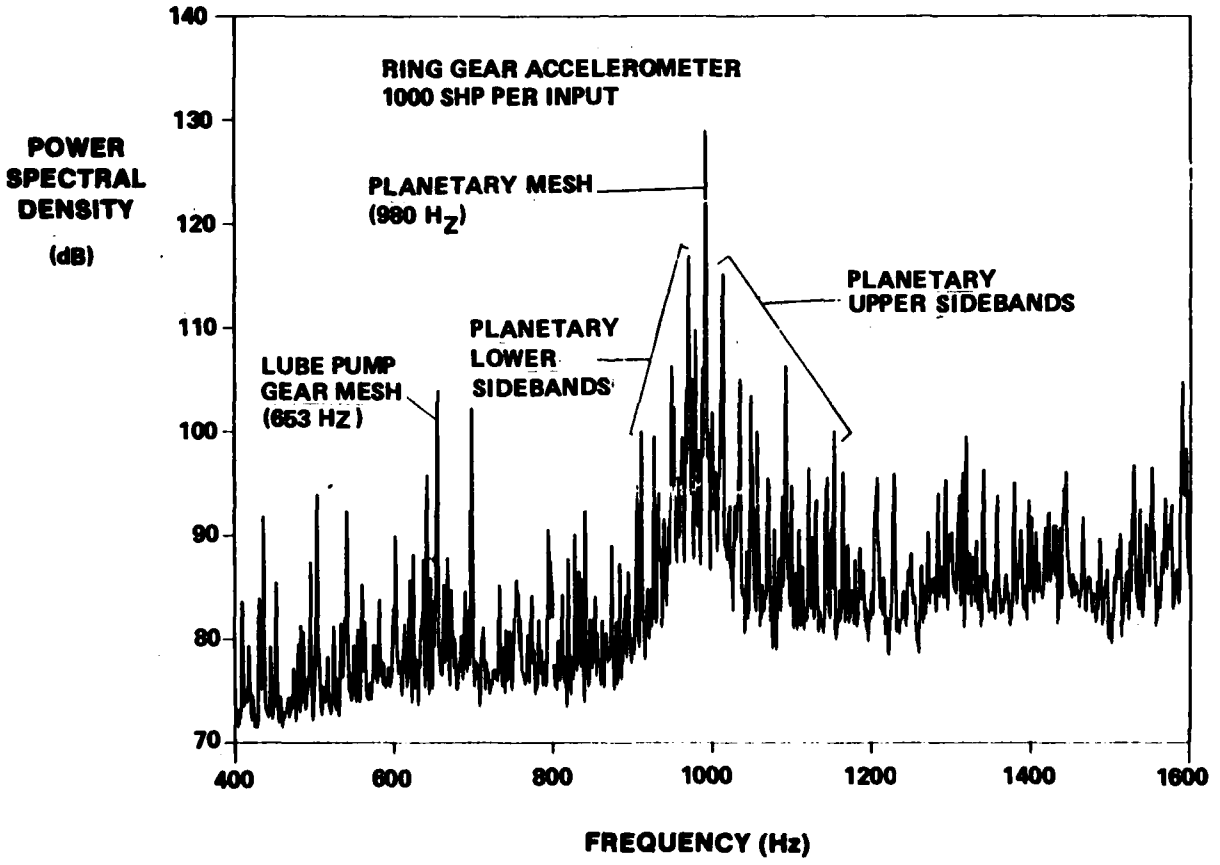

Figure 30. Baseline Gearbox Acceleration Levels.

WIDE BAND LEVELS

Wide band power spectral density (PSD) plots are shown in Figures 31 through 37 for the four experimental configurations and the production gearbox. Plotted data were taken at 100% speed and 1000 HP per input (test condition 9), selected as typical of normal cruise conditions for the BLACK HAWK. For the two configurations with the magnesium housing (Figures 31 through 34), plots include the housing sidewall, right input gear bearings, tail takeoff bearings, left combining pinion bearing and ring gear. For the two configurations with the stainless steel housing (Figures 35 and 36), housing sidewall readings were not taken because the accelerometer mount could not withstand the vibration levels. Plots for the right input gear bearings with the stainless steel housing were omitted since they were essentially the same as those shown for the magnesium housing (input housings were magnesium in all tests).

These auto spectrum plots of acceleration signals are representative of data taken from all accelerometer locations at this test condition. The plots show vibratory response of each accelerometer to dynamic excitations over a frequency band of 0-6000 Hz, vibratory response of each of the test configurations, and relative vibration levels for each excitation. The PSD reference is $10^{-6}g^2/Hz$ for Figures 31 through 37.

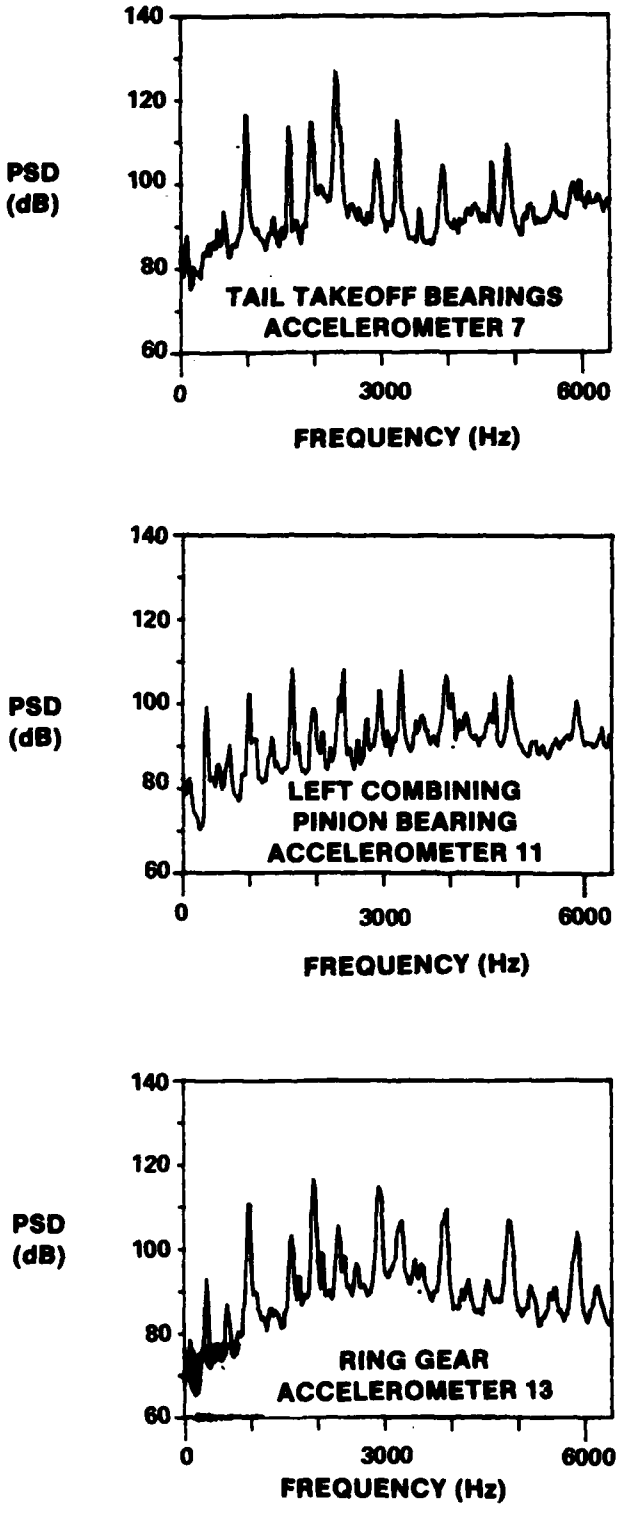

Figure 31. Baseline Gearbox PSD (Sheet 1).

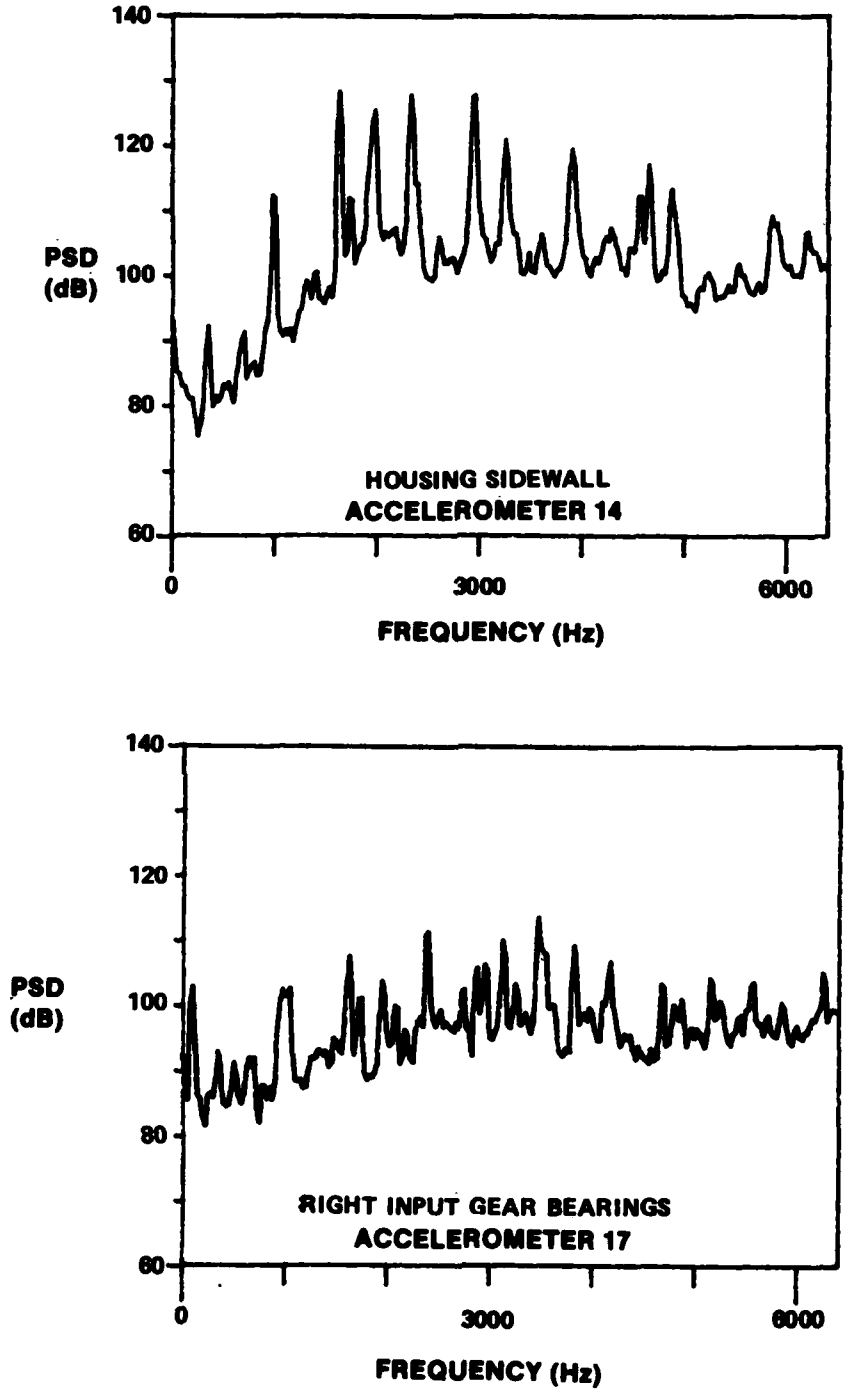

Figure 32. Baseline Gearbox PSD (Sheet 2).

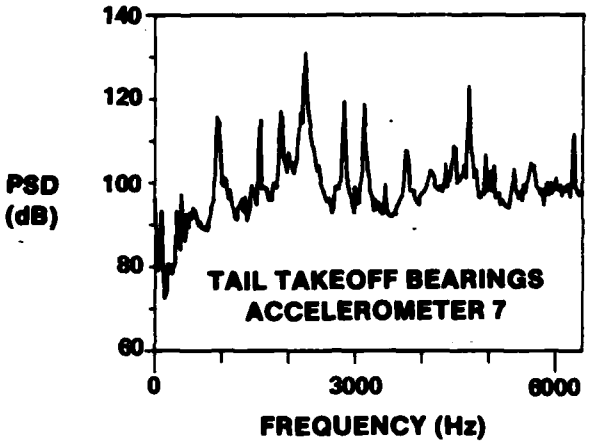

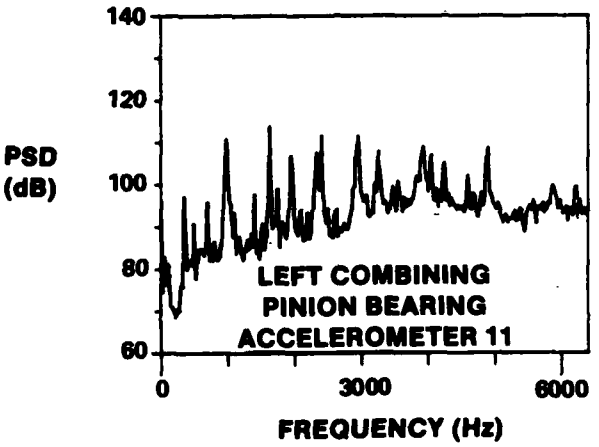

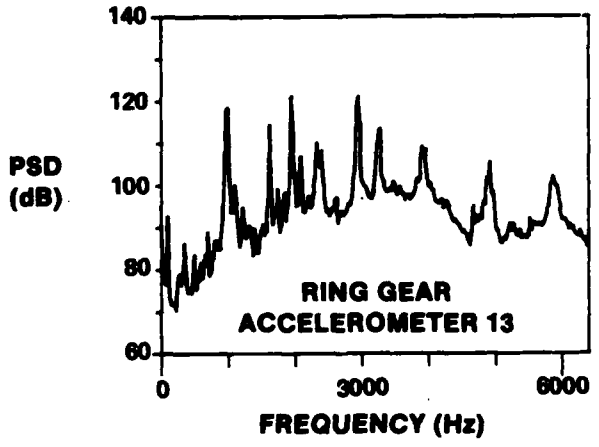

Figure 33. HCR Planetary PSD (Sheet 1).

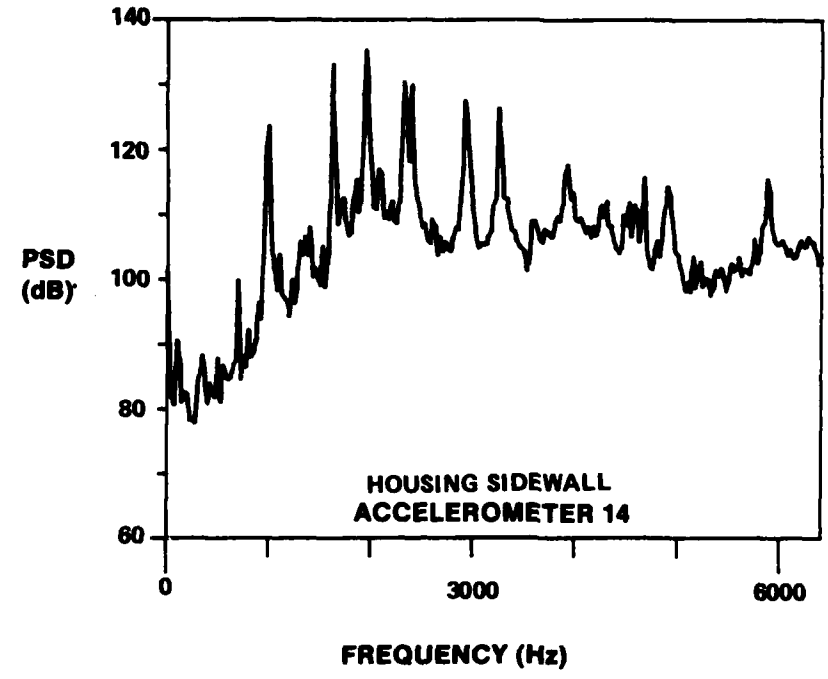

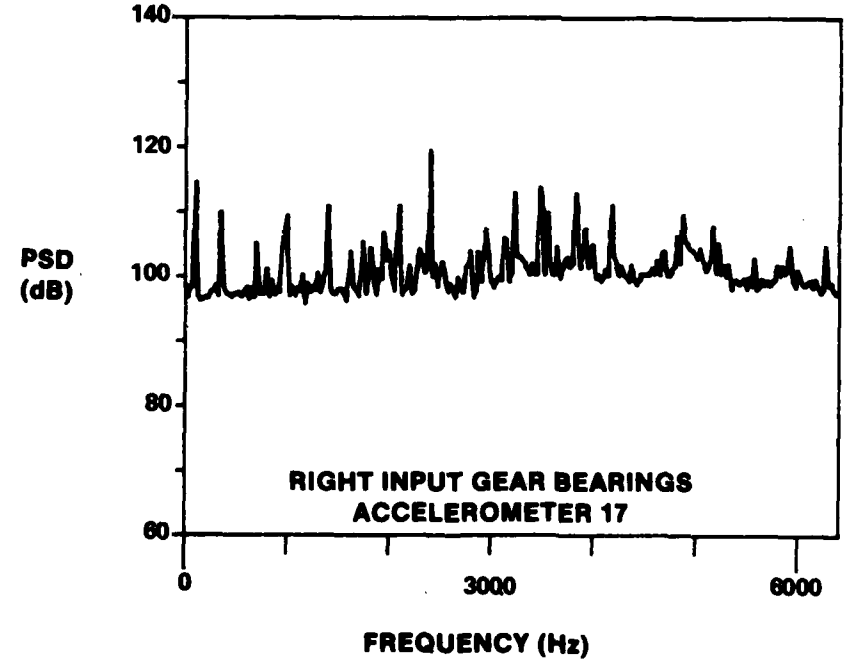

Figure 34. HCR Planetary PSD (Sheet 2).

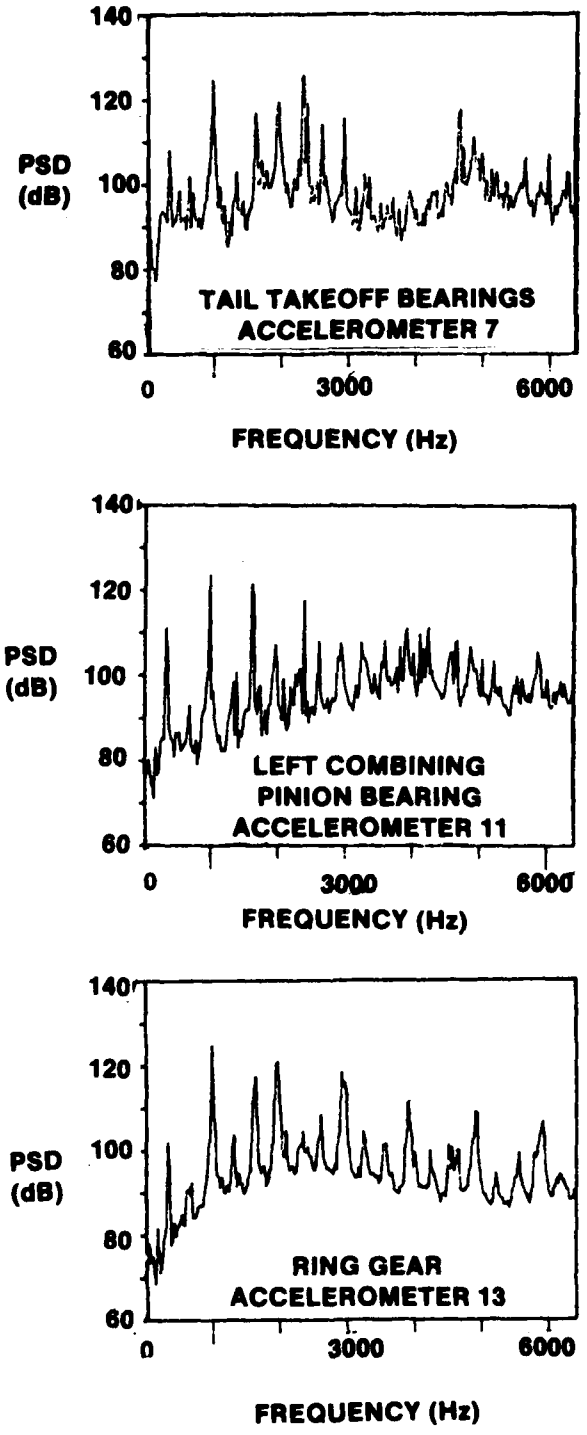

Figure 35. Steel Housing PSD.

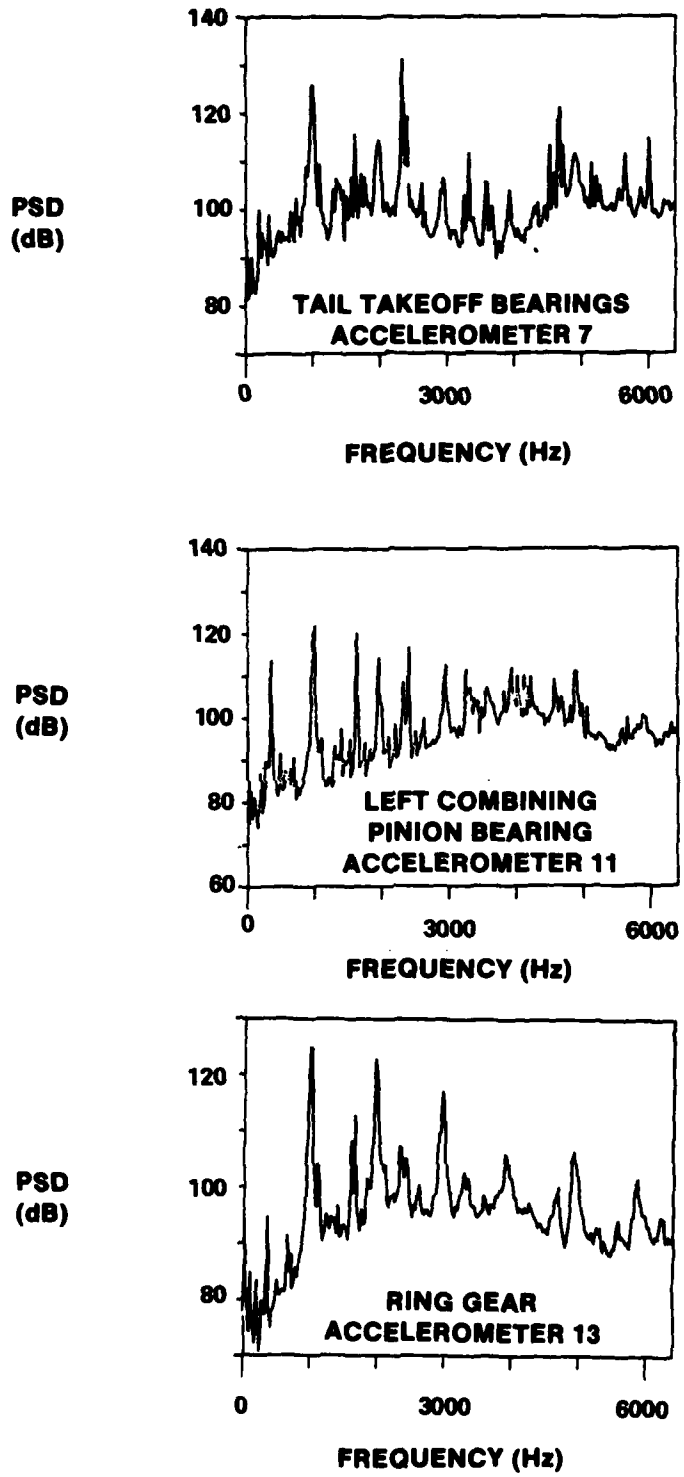

Figure 36. Steel Housing and HCR Planetary PSD.

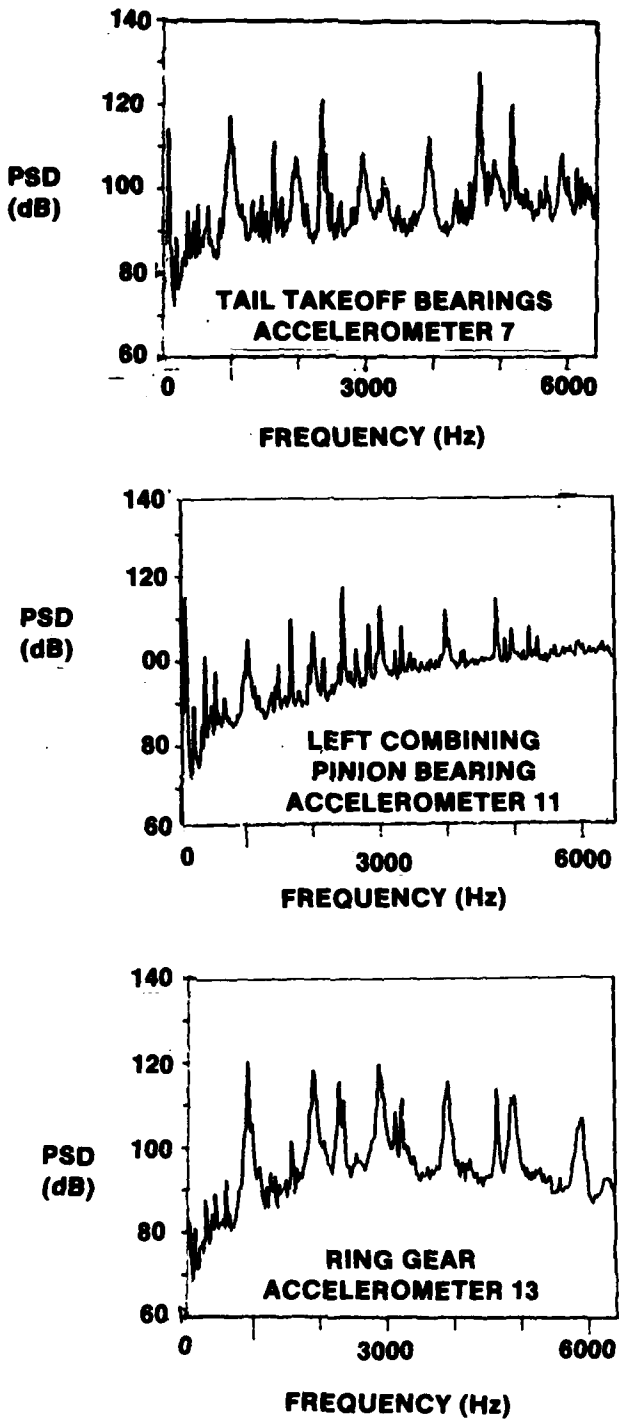

Figure 37. Production Gearbox PSD.

EFFECTS OF POWER AND SPEED

Speed and load sensitivities based on ring gear accelerometer data for each configuration were plotted for the planetary mesh frequency (980 Hz) and two times the planetary mesh frequency (1960 Hz). Figure 38 shows auto spectrum plots of acceleration signals at the planetary mesh frequency. Figures 39 through 43 compare power and speed for various combinations of test gearbox configurations and excitation frequencies. By choosing a constant reference (100% of main rotor speed), the variation of vibration levels were plotted as a function of planetary horsepower only (Figures 38 and 39). These figures show vibratory power levels contained in a 125-Hz band about the central frequency. This bandwidth includes 28 main rotor shaft modulation sidebands (14 below and 14 above) around the planetary mesh frequency. This provides a good representation of all the energy contained in the planetary mesh and its sidebands since the sideband levels are approximately 20-30 dB lower than the peak at the edges of this bandwidth. The levels shown are determined from

$$\text{Power} = \int_{\omega_1}^{\omega_2} \text{PSD}\, dw \qquad (7)$$

where $\omega_2 - \omega_1 = 125$ Hz

and $\frac{\omega_1 + \omega_2}{2}$ = planetary mesh frequency (or twice mesh frequency)

The PSD reference is 10^{-6} g for Figures 38-43.

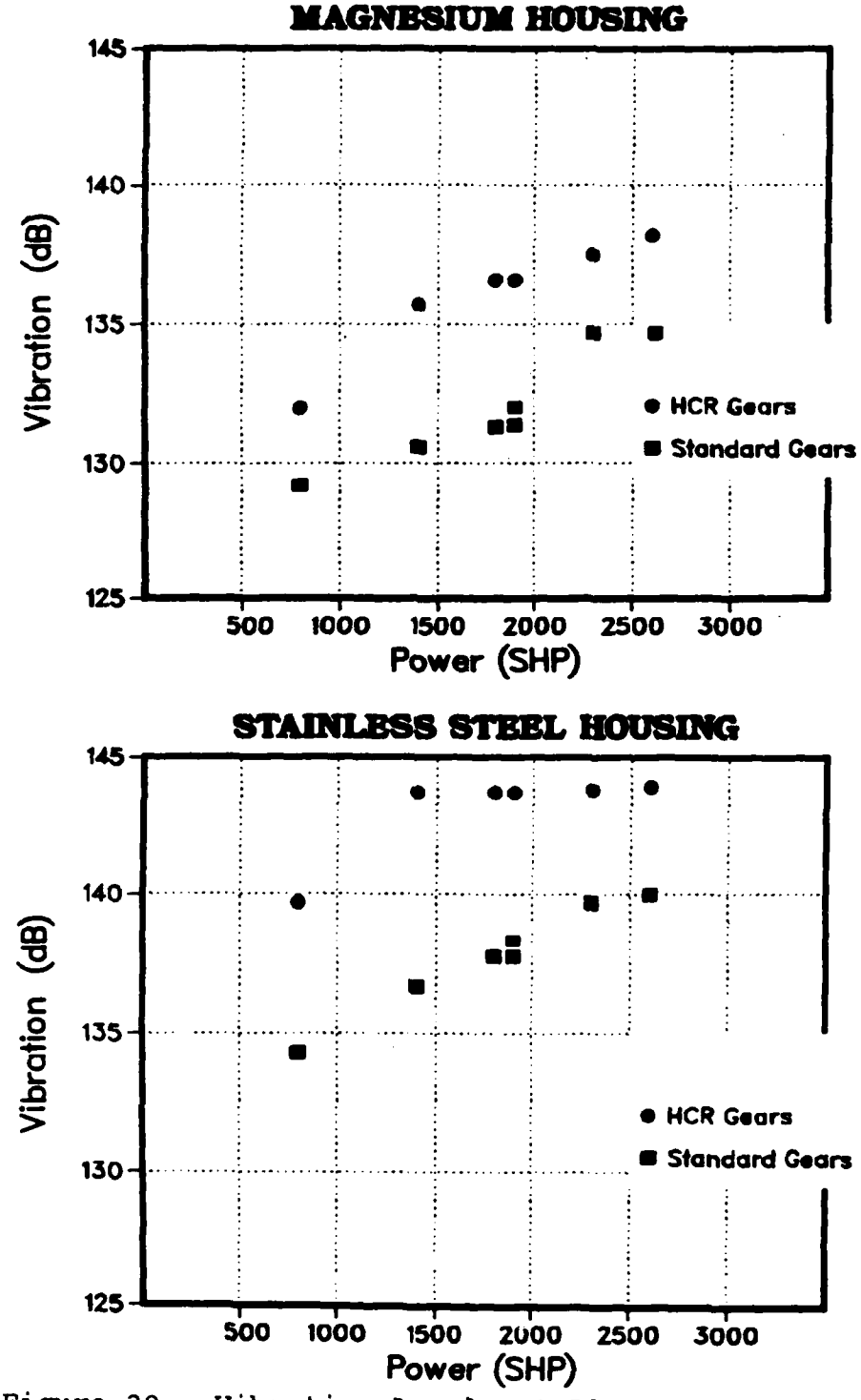

Figure 38. Vibration Levels at Planetary Mesh (Comparing Planetaries).

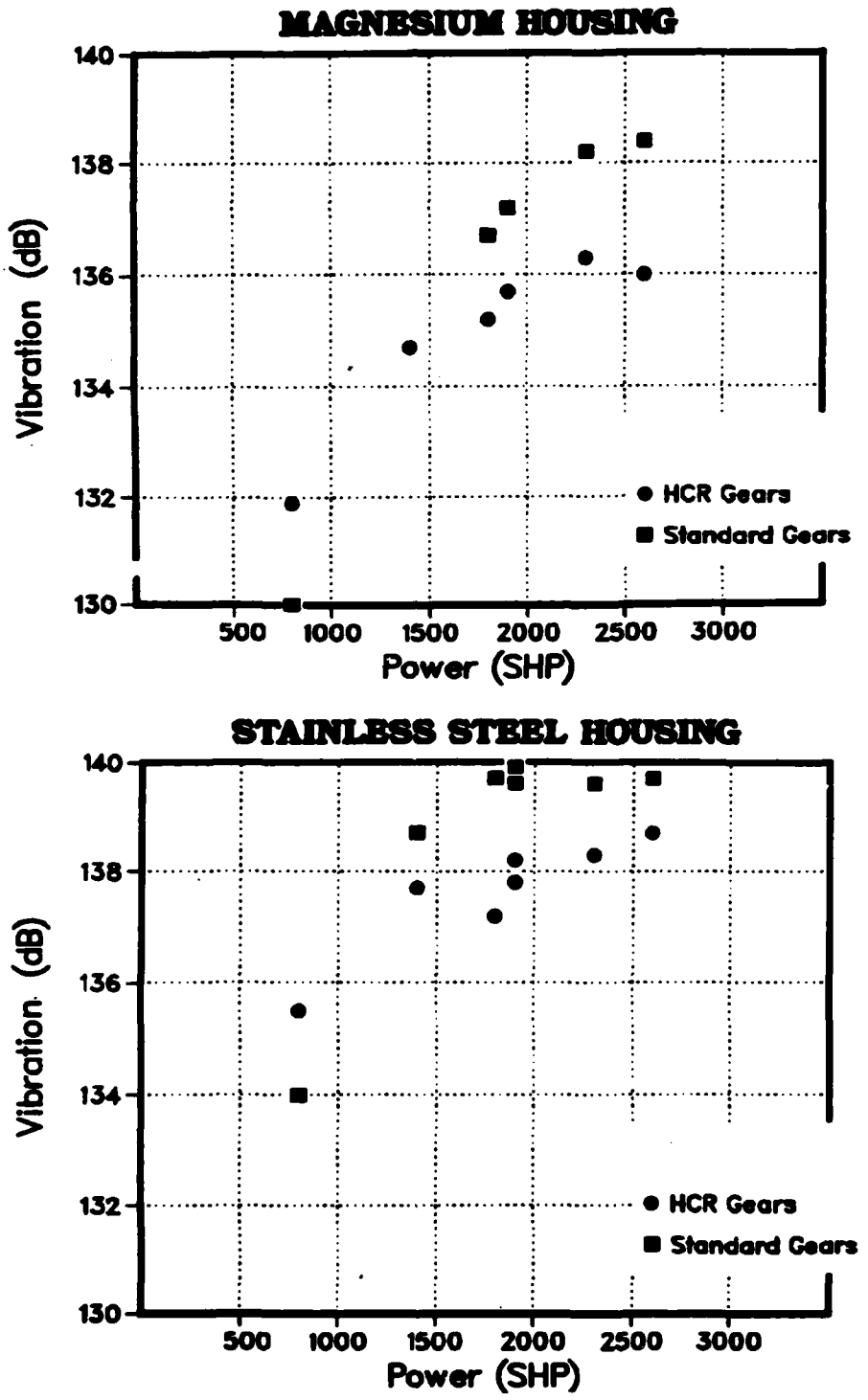

Figure 39. Vibration Levels at 2X Planetary Mesh (Comparing Planetaries).

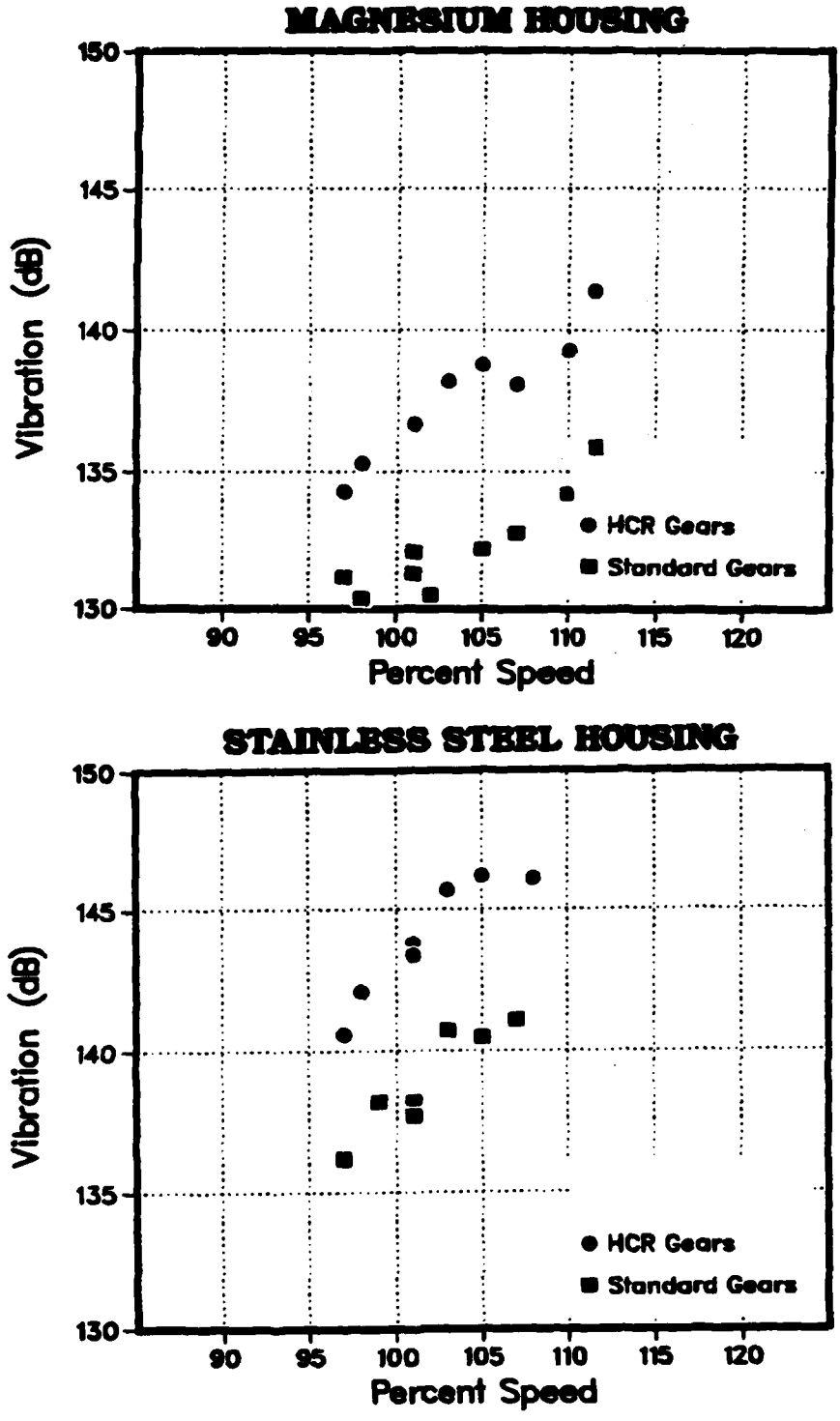

Figure 40. Vibration Levels at Planetary Mesh (2000 SHP).

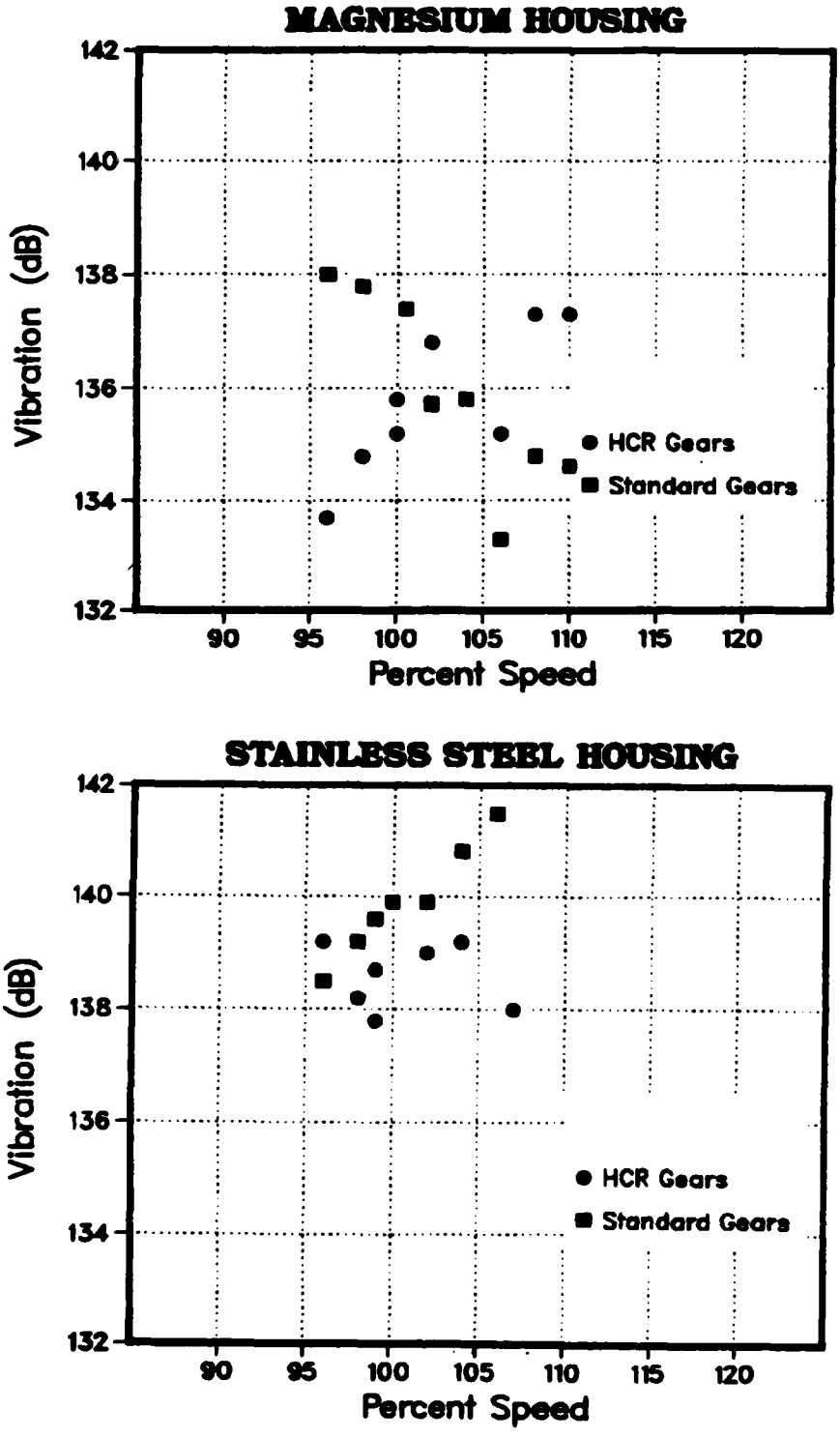

Figure 41. Vibration Levels at 2X Planetary Mesh (2000 SHP).

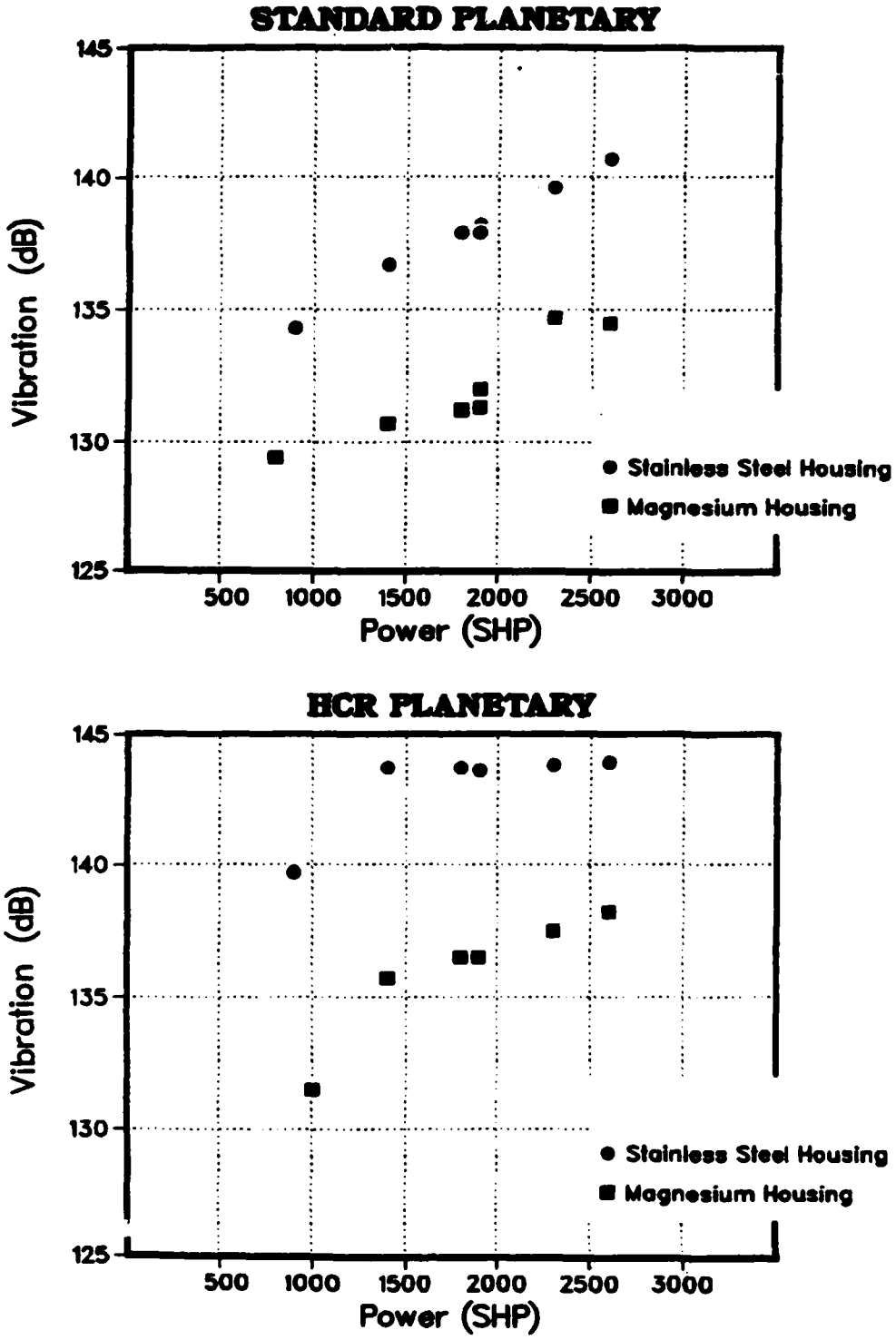

Figure 42. Vibration Levels at Planetary Mesh (Comparing Housings).

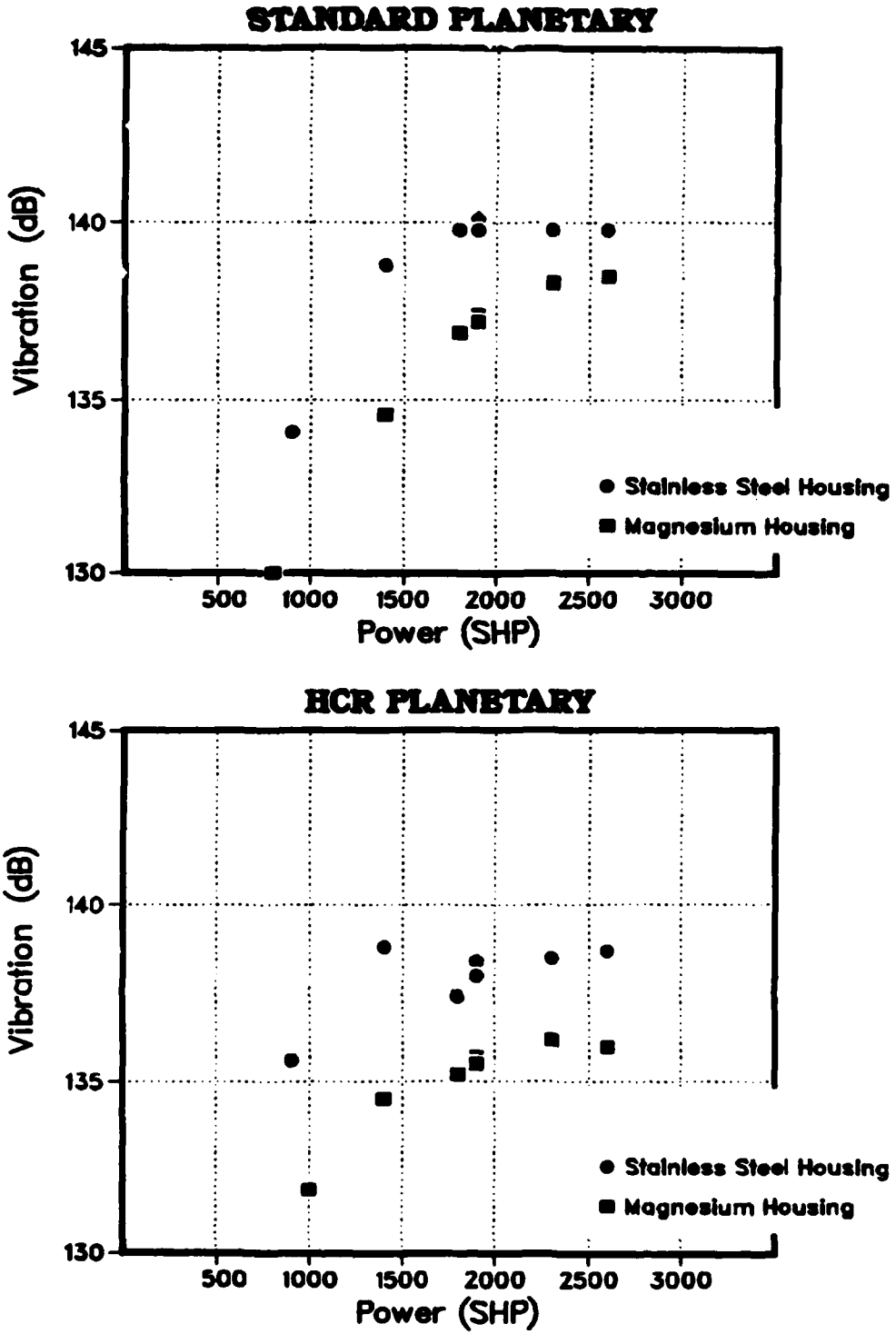

Figure 43. Vibration Levels at 2X Planetary Mesh (Comparing Housings).

NARROW BAND LEVELS

The last set of vibration plots are narrow band plots of the power spectral density (PSD) from the ring gear accelerometer. Figures 44 and 45 show the acceleration levels for the narrow band range of 800 to 1200 Hz for the first four test configurations. The relative repeatability of gearbox vibration is shown in Figure 46, where the baseline data (from Figure 44) is compared to data from a production gearbox; vibration levels are comparable, with variations as expected from gearbox to gearbox. In this frequency range the planetary mesh frequency is clearly dominant. Associated with the mesh frequency are its sidebands, which occur at multiples of various forcing frequencies. Sideband frequencies are calculated as follows (the theory is discussed in subsection entitled Explanation of Sidebands).

$$f_{sb} = f_{pm} \pm n\,(f_f) \qquad (8)$$

where f_{sb} = sideband frequency

f_{pm} = planetary mesh frequency

$\pm n$ = upper or lower sideband multiple integers ($n = 1,2,3\ldots$)

f_f = forcing frequency of modulation source

Table 7 lists the significant sidebands for the planetary mesh frequency.

Table 7. PLANETARY MESH SIDEBAND FREQUENCIES

	Sideband Frequencies (Hz)		
n	Output Shaft/ Planet Carrier	Planet Pass (5x Carrier)	Sun Gear
-10	937.0	765.0	779.0
-5	958.5	872.5	879.5
-2	971.4	937.0	939.8
-1	975.7	958.5	959.9
0	980.0	980.0	980.0
1	984.3	1001.5	1000.1
2	988.6	1023.0	1020.2
5	1001.5	1087.5	1080.5
10	1023.0	1195.0	1181.0

The predominant sidebands are caused by multiples of five (number of planet gears) times the planet carrier frequency, which is the planet pass frequency; this is the rate at which the planet gears pass the fixed accelerometer location on the ring gear (sidebands developed at 980 ±n (21.5) Hz). When the mesh is directly under the accelerometer, the noise is loudest. Since the accelerometer is nearest the planet-ring gear mesh, the highest sideband is expected there. What is surprising is that the sun gear rotational modulation effects are also present (sidebands developed at 980 ±n (20.1) Hz). Planet pass modulation cannot be eliminated; however, with an extremely accurate sun gear and no eccentricity of rotation, the sun rotational effects on sidebanding can be minimized. There appears also to be modulation caused by the output shaft/planet carrier rotation (sidebands at 980 ±n (4.3) Hz). The PSD reference for Figures 44 thru 46 is $10^{-6} g^2/Hz$.

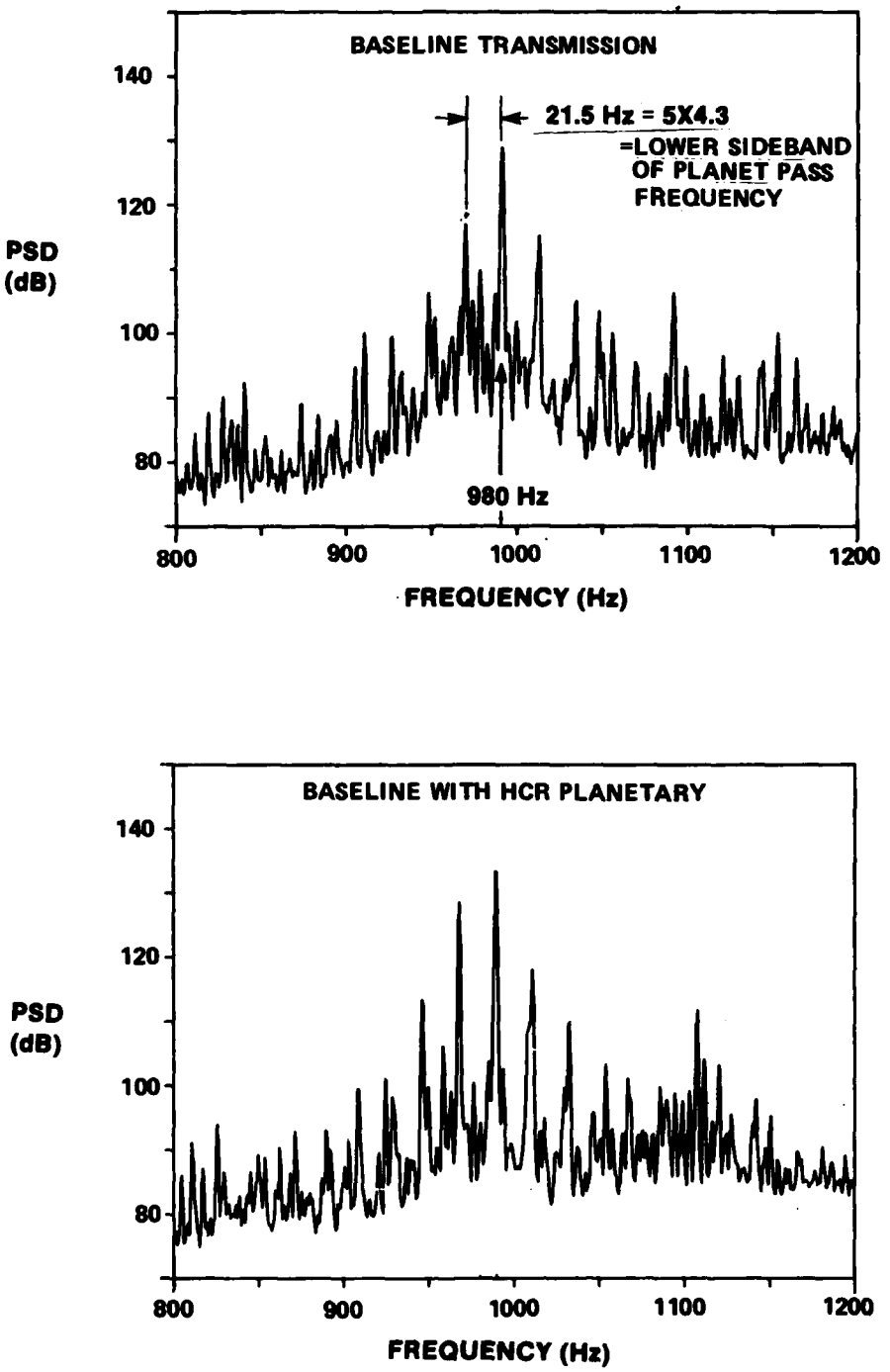

Figure 44. Narrow Band Acceleration Levels (Magnesium Housing).

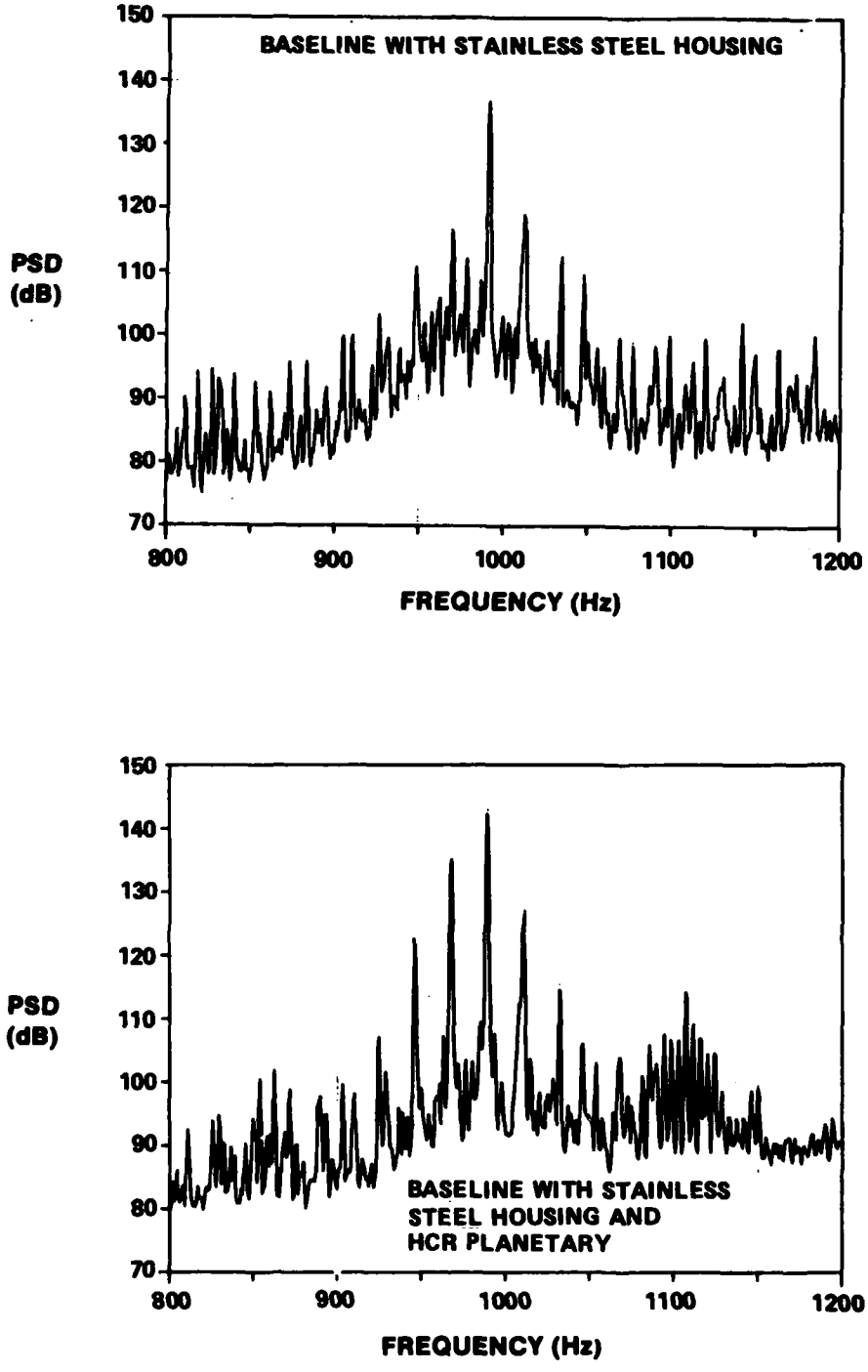

Figure 45. Narrow Band Acceleration Levels (Steel Housing).

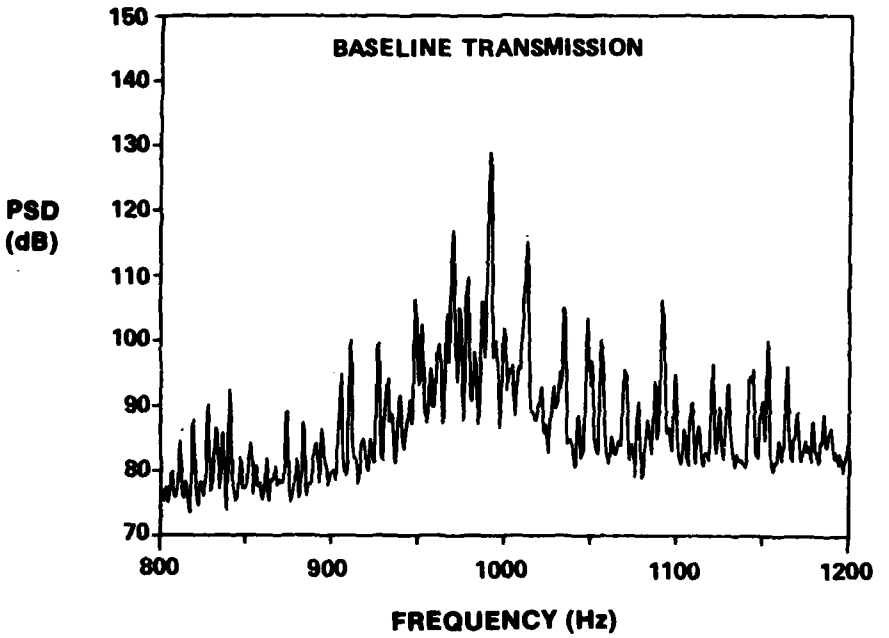

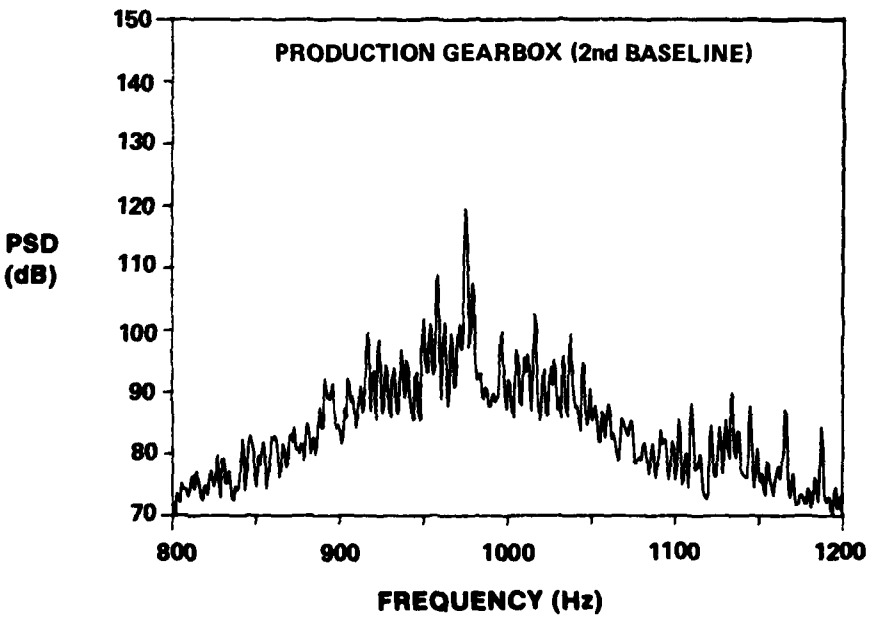

Figure 46. Narrow Band Acceleration Level Repeatability.

EXPLANATION OF SIDEBANDS

For geared systems, there are often strong vibration components at frequencies surrounding the gear mesh frequency and its harmonics. These sideband frequencies result from amplitude modulation and/or frequency modulation of the basic mesh frequency (Reference 3).

Amplitude modulation occurs when the excitation varies in amplitude with time even though the frequency is constant. In its simplest form, a once-per-revolution gear eccentricity would cause amplitude modulation with the following results:

$$A(t) = A_o(1 + e \sin \omega_s t) \sin \omega_m t \tag{9}$$

where ω_m is the basic mesh frequency, ω_s is the sideband frequency, and the factor in parentheses represents the eccentric modulation at shaft frequency superimposed on the basic mesh frequency. This can be expanded in the form

$$A(t) = A_o \sin \omega_m t + \tfrac{1}{2} A_o e [\cos (\omega_m - \omega_s)t - \cos (\omega_m + \omega_s)t] \tag{10}$$

Notice that even this simple case produces three frequencies: ω_m, $\omega_m - \omega_s$, and $\omega_m + \omega_s$. The first, ω_m, is the fundamental mesh frequency, while the second and third are the lower and upper sideband frequencies. In general, the modulation is not a simple, once-per-revolution sinusoid but has a complex waveform which can be decomposed into a Fourier series related to shaft revolution and its higher harmonics (smaller shaft angle rotations representing shorter spatial distances):

$$A(t) = A_o[1 + \sum_{k=1}^{\infty} \alpha_k \sin (k\omega_s t + \gamma_k)] \sin \omega_m t \tag{11}$$

The expansion of this Fourier series takes the form

$$A(t) = A_o \sin\omega_m t + \tfrac{1}{2} A_o \sum_{k=1}^{\infty} \{\alpha_k (\cos[(\omega_m - k\omega_s)t - \gamma_k] - \cos [(\omega_m + k\omega_s)t + \gamma_k])\} \tag{12}$$

This shows that amplitude modulation produces sidebands at all multiples of shaft speed about the mesh frequency on both the lower $(\omega_m - k\omega_s)$ and the upper $(\omega_m + k\omega_s)$ sides.

3. Smith, J.D., Gears And Their Vibration, The Macmillan Press Limited, 1983.

Frequency modulation occurs when the mesh frequency changes with time. Even under constant shaft speed conditions, this will occur because of the influence of parameters such as gear tooth variation, torsional vibration of the entire gear train, drive motor speed fluctuations, and rotor load fluctuations. The simplest case can be formulated as

$$A(t) = A_o \sin \left[\omega_m t + \frac{\Delta\omega}{\omega_s} \sin (\omega_s t + \beta)\right] \qquad (13)$$

which will produce an infinite number of sideband frequencies at $\omega_m \pm k\omega_s$ (where $k = 0,1,2,3....$). This has the potential of producing sideband levels which are higher than the fundamental mesh frequency level.

PLANETARY GEARSET VARIATION

To help understand the effects of gear tooth manufacturing errors on acoustical vibration, the HCR gears were reinspected after testing; these gears showed no signs of wear, so any wear which may have occurred during testing was negligible.

The following gear tooth variations (Reference 4) were measured:

Pitch Variation	Distance of tooth from its theoretical position.
Spacing Variation	Difference in the pitch variation of two adjacent teeth.
Index Variation	Accumulation of pitch variation.
Profile Error	Deviation of the tooth profile from true involute form.
Lead Error	Deviation along the tooth face.

The difference between pitch and spacing variation is illustrated in Figure 47.

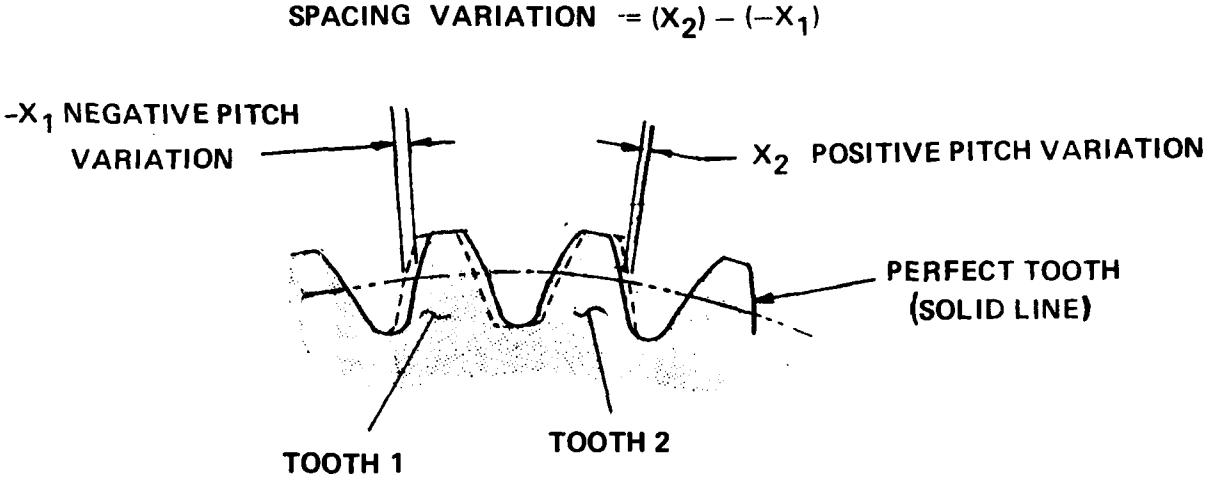

Figure 47. Tooth Pitch and Spacing Variations.

4. AGMA Gear Handbook, Volume 1, March 1980, (P390.03) Gear Classification, Materials and Measuring Methods for Unassembled Gears.

Figures 48 through 59 are the gear manufacturing charts for the HCR sun gear, ring gear, and a planet gear chosen at random. The manufacturing charts shown are for lead, profile, pitch, spacing, and index variations. Both pitch variation and spacing variations are important parameters for high contact ratio gear teeth because they relate to load sharing. Charts for the baseline (production) planetary were not developed; however, inspection sheets were examined and are summarized in Table 8.

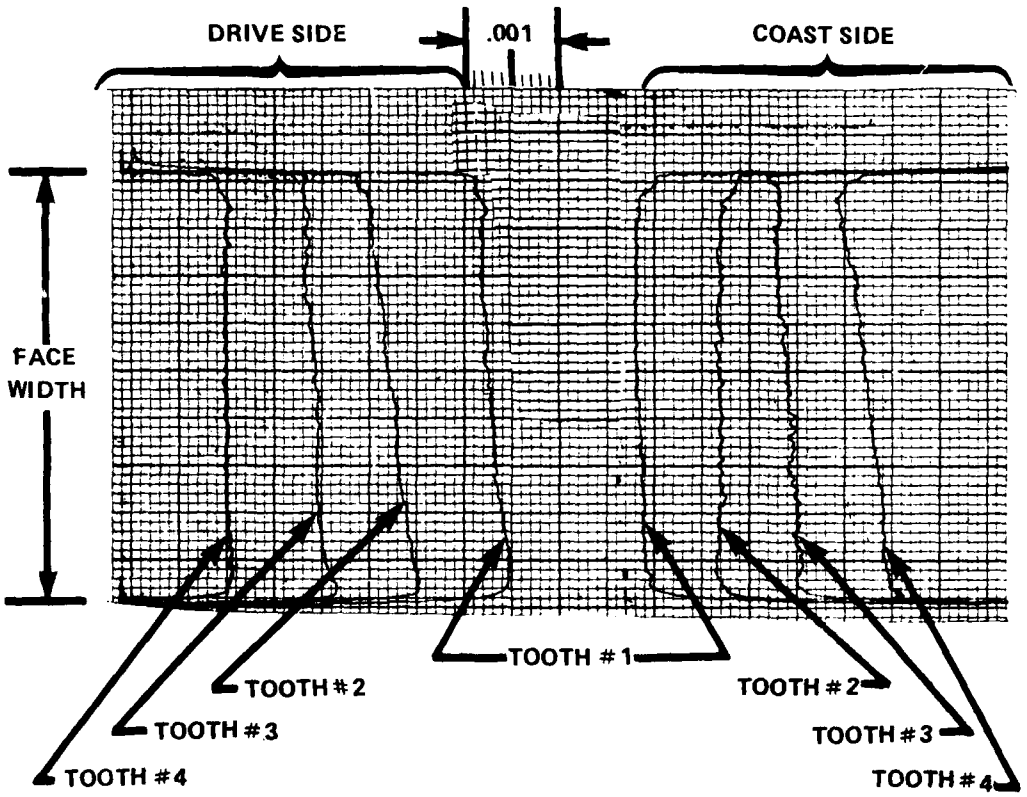

Figure 48. HCR Sun Gear Lead.

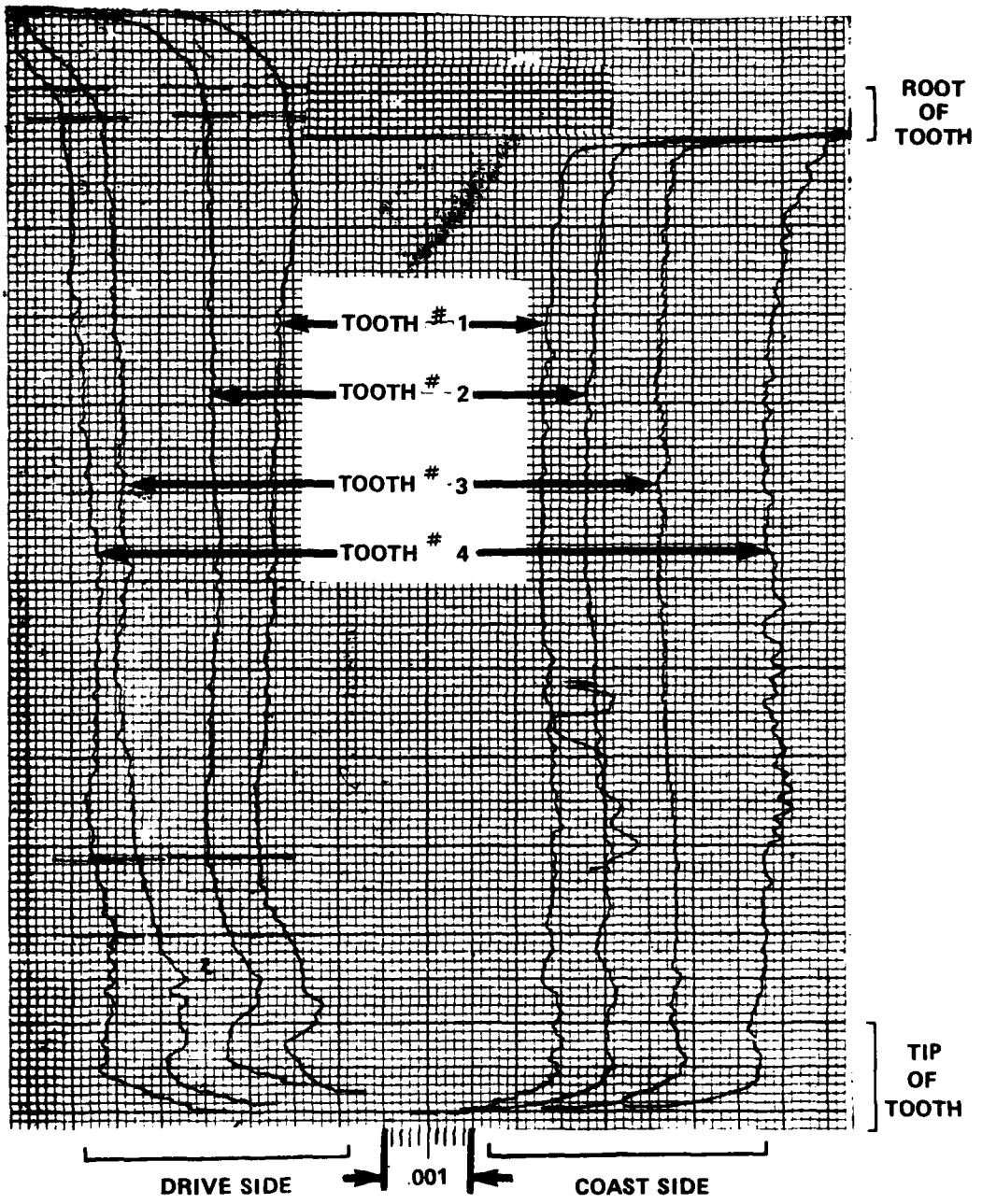

Figure 49. HCR Sun Gear Profile.

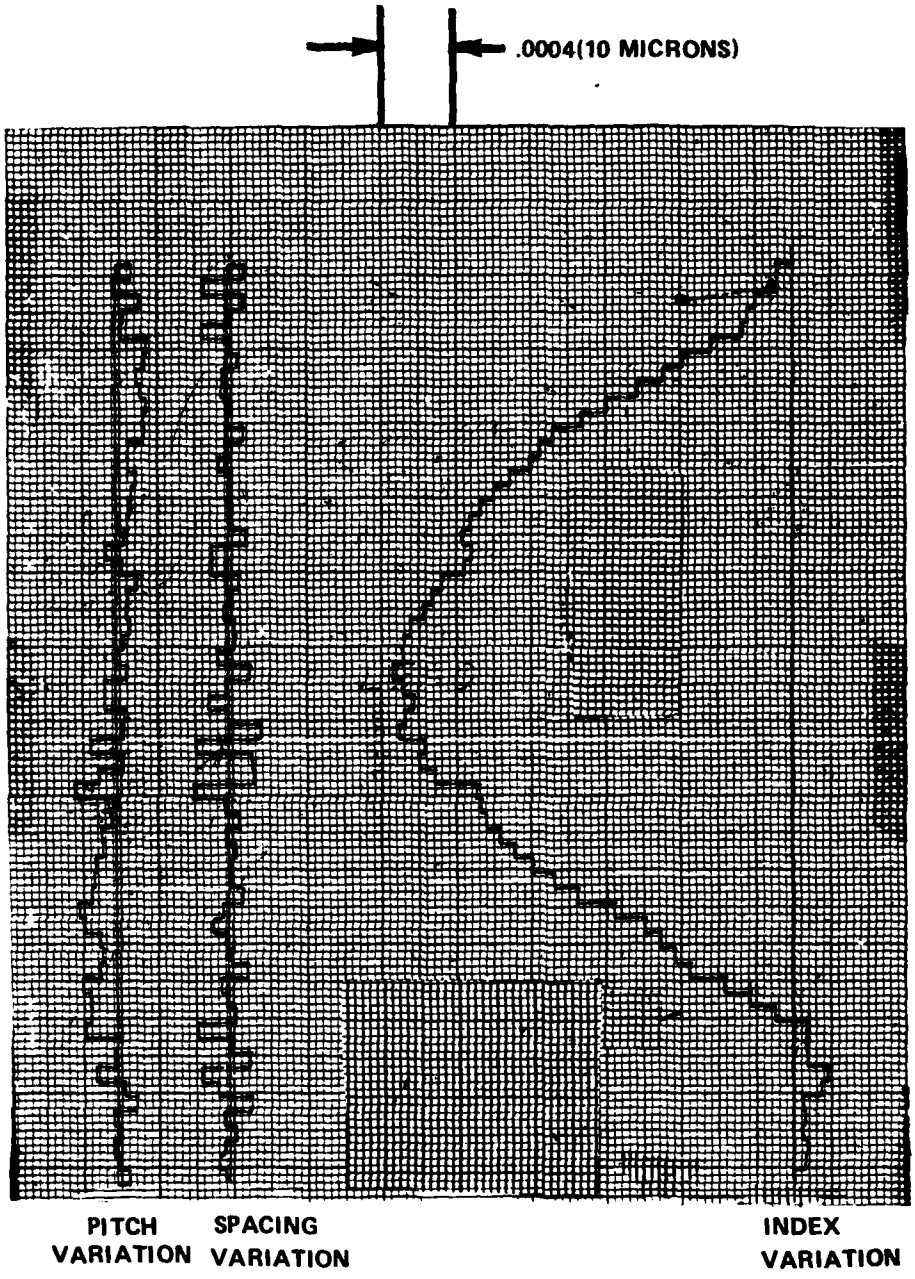

Figure 50. HCR Sun Gear Pitch, Spacing, and Index (Drive Side).

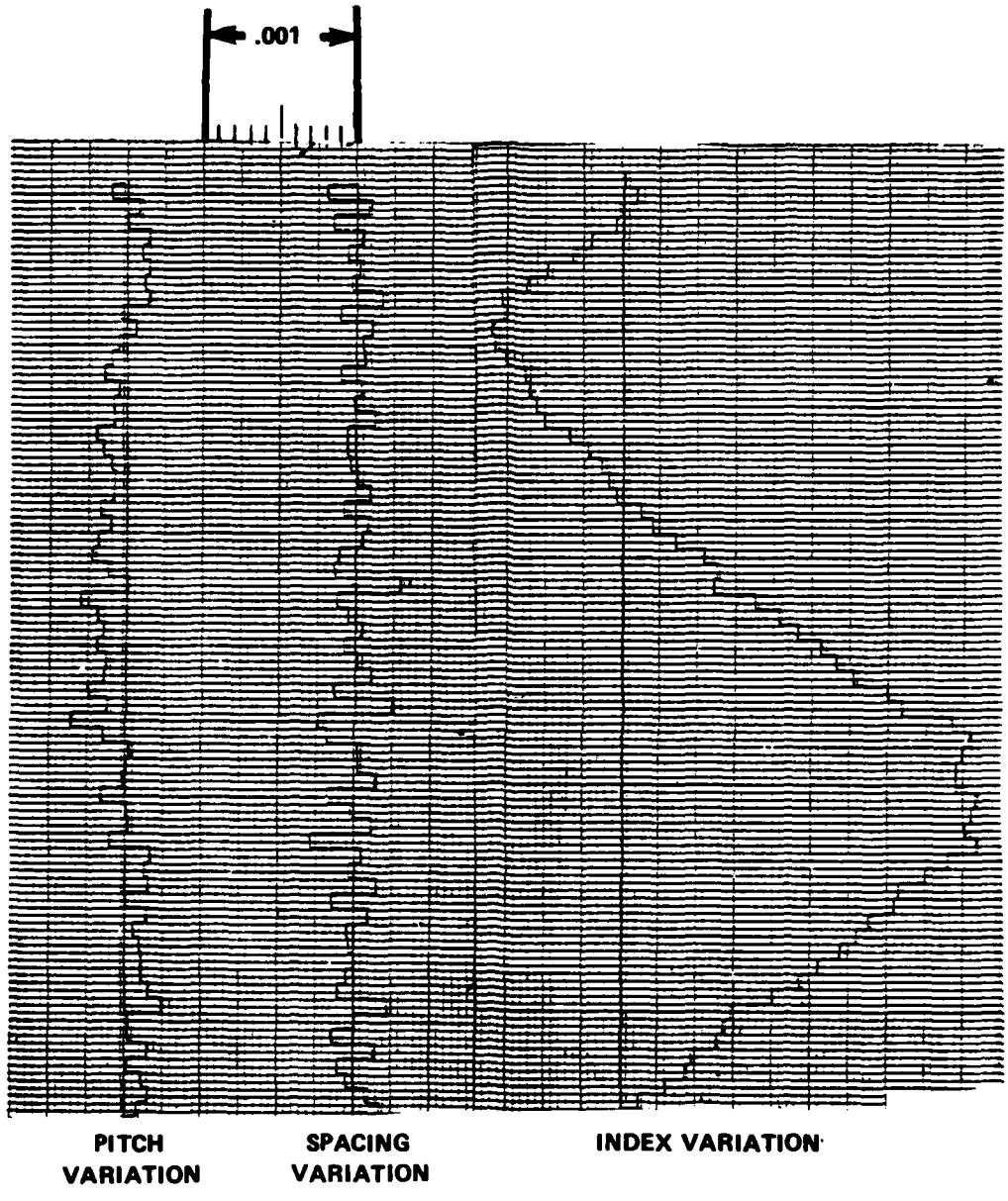

Figure 51. HCR Sun Gear Pitch, Spacing and Index (Coast Side).

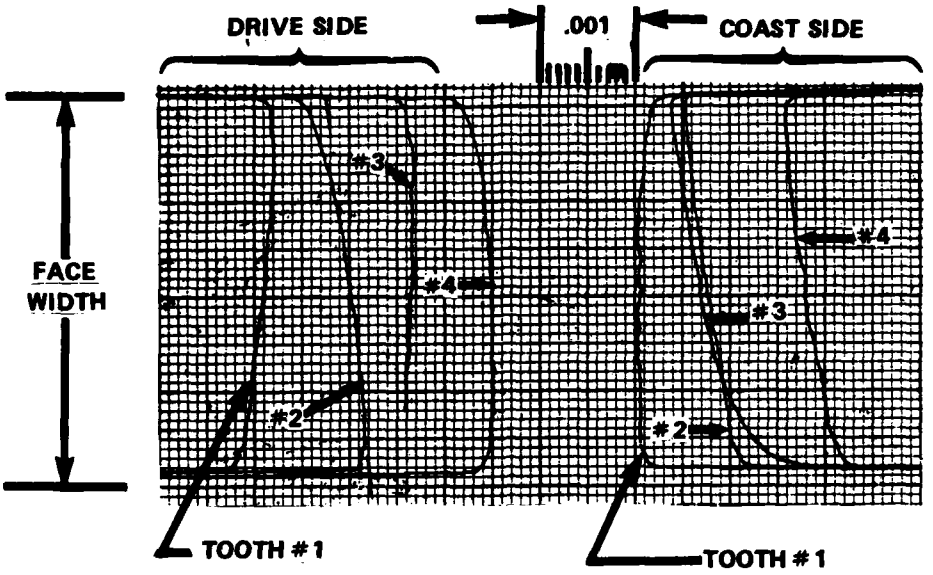

Figure 52. HCR Ring Gear Lead.

10
F

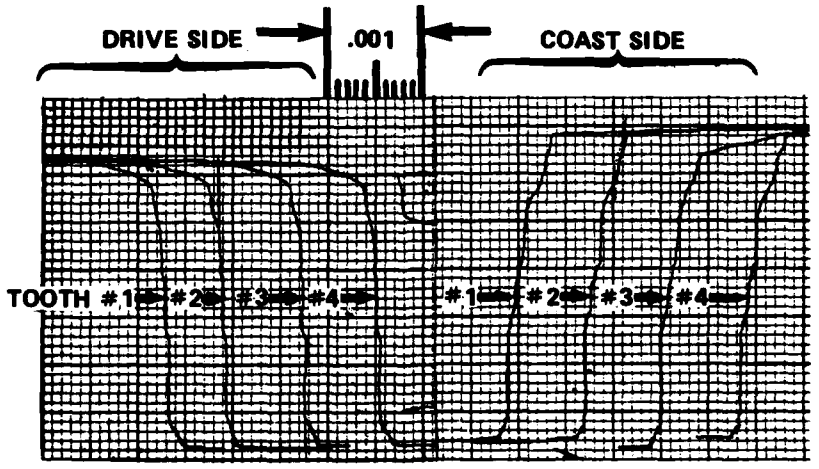

Figure 53. Ring Gear Profile.

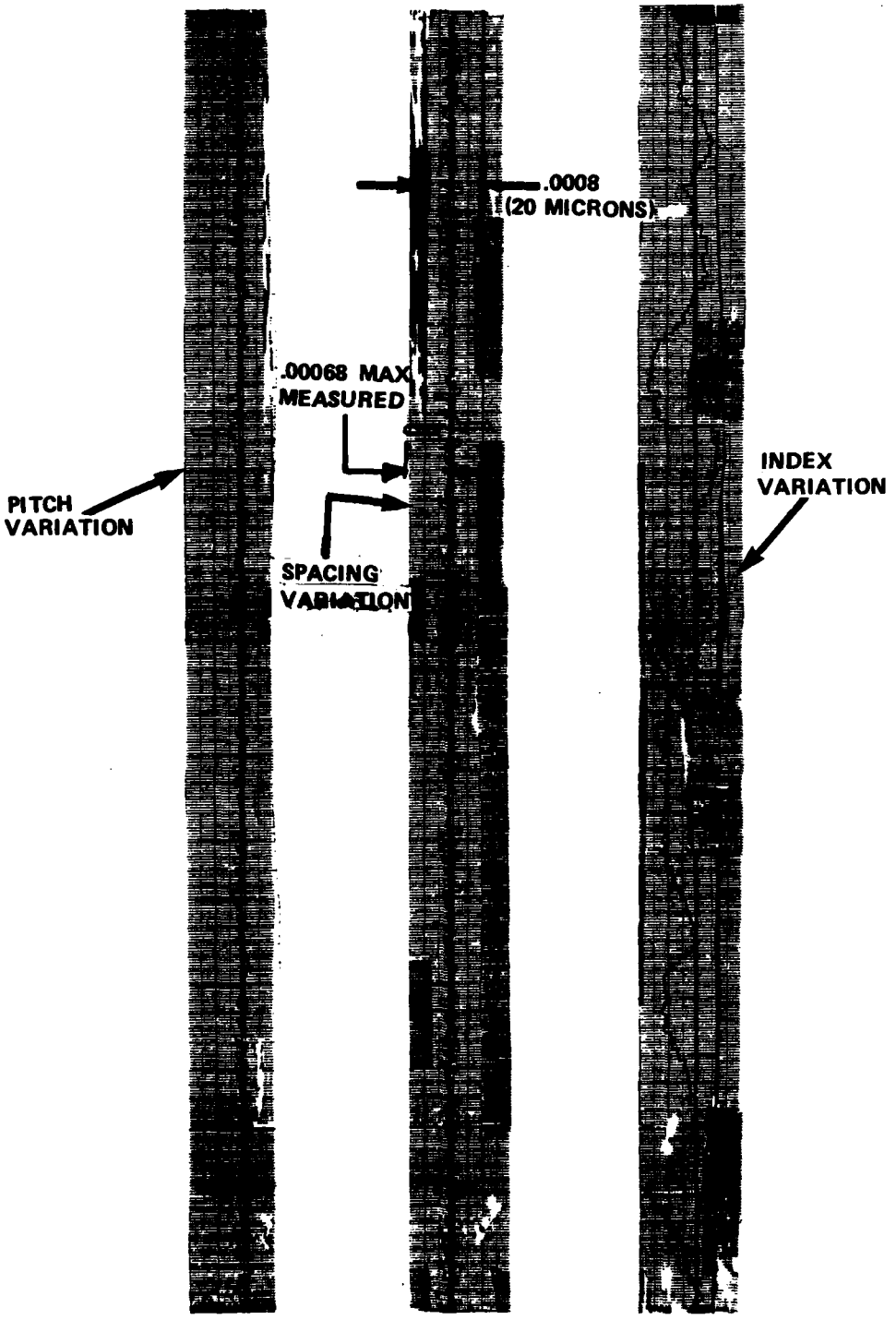

Figure 54. HCR Ring Gear Pitch, Spacing and Index (Drive Side).

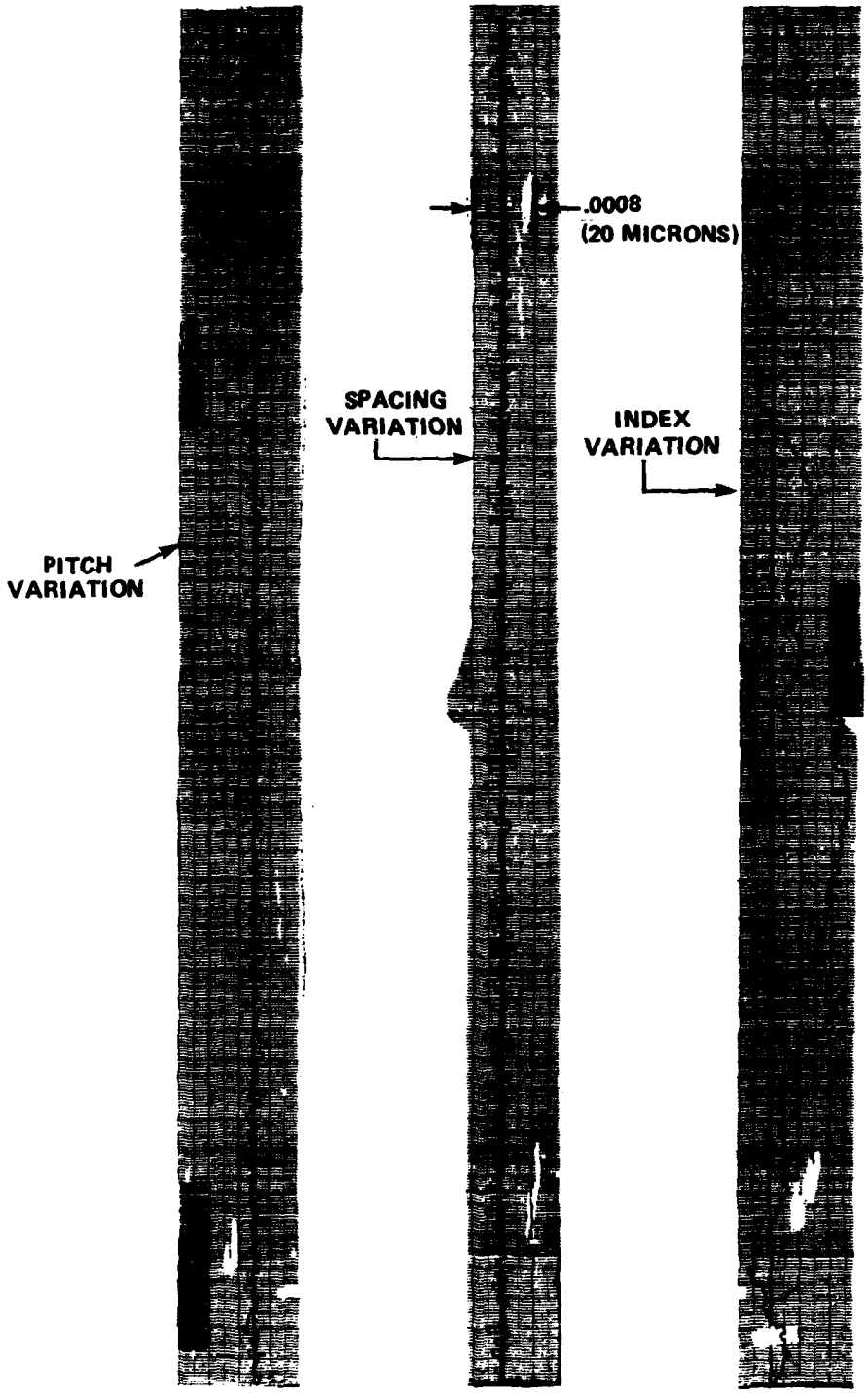

Figure 55. HCR Ring Gear Pitch, Spacing and Index (Coast Side).

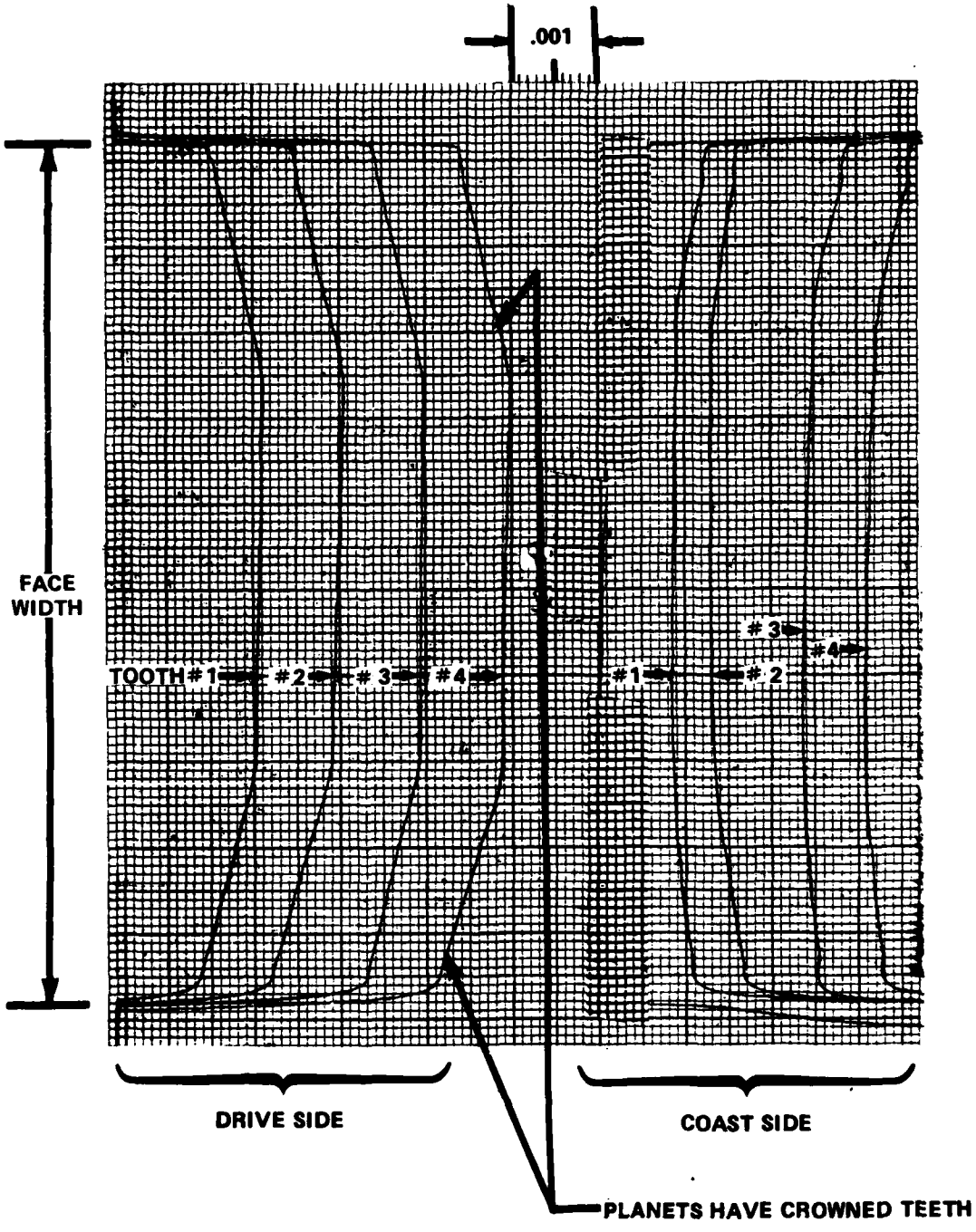

Figure 56. HCR Planet Gear Lead.

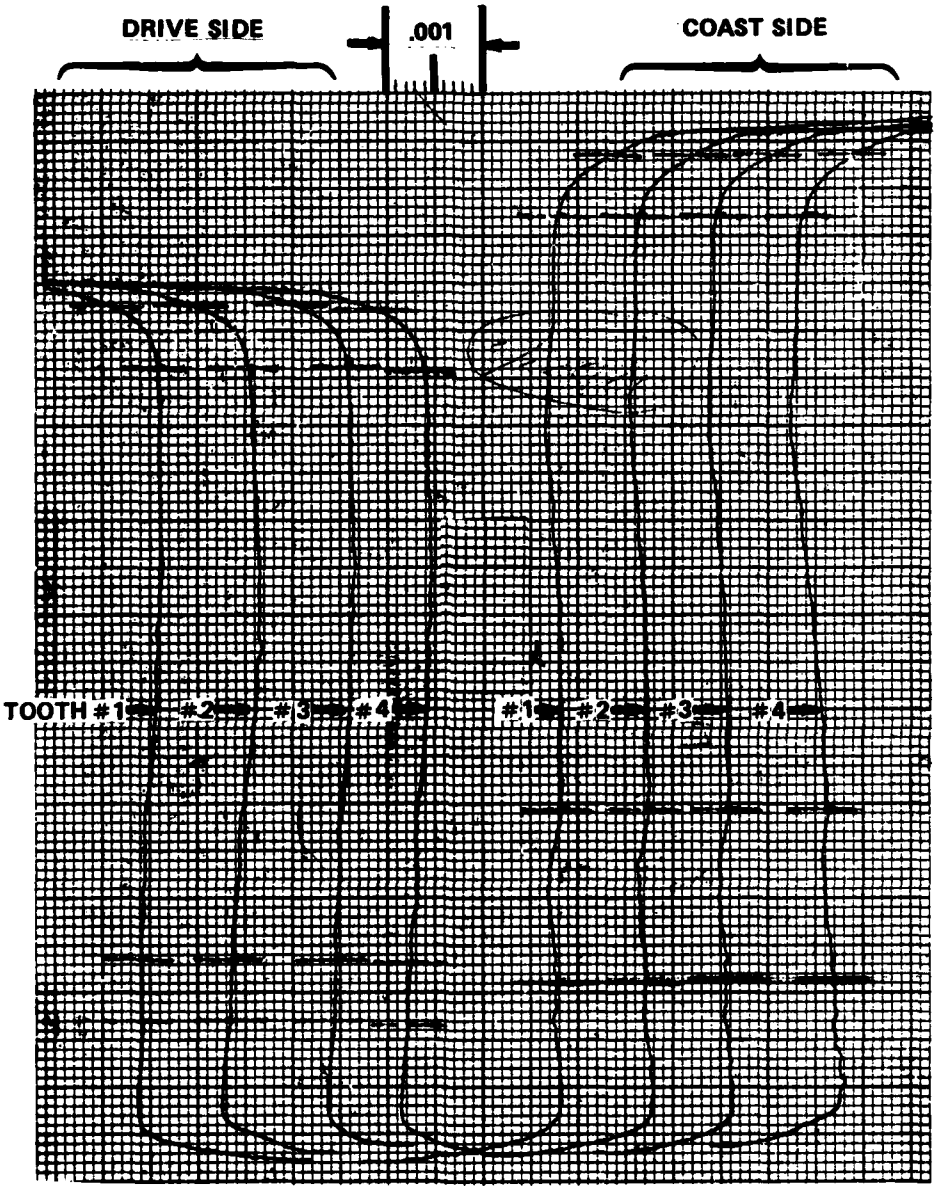

Figure 57. HCR Planet Gear Profile.

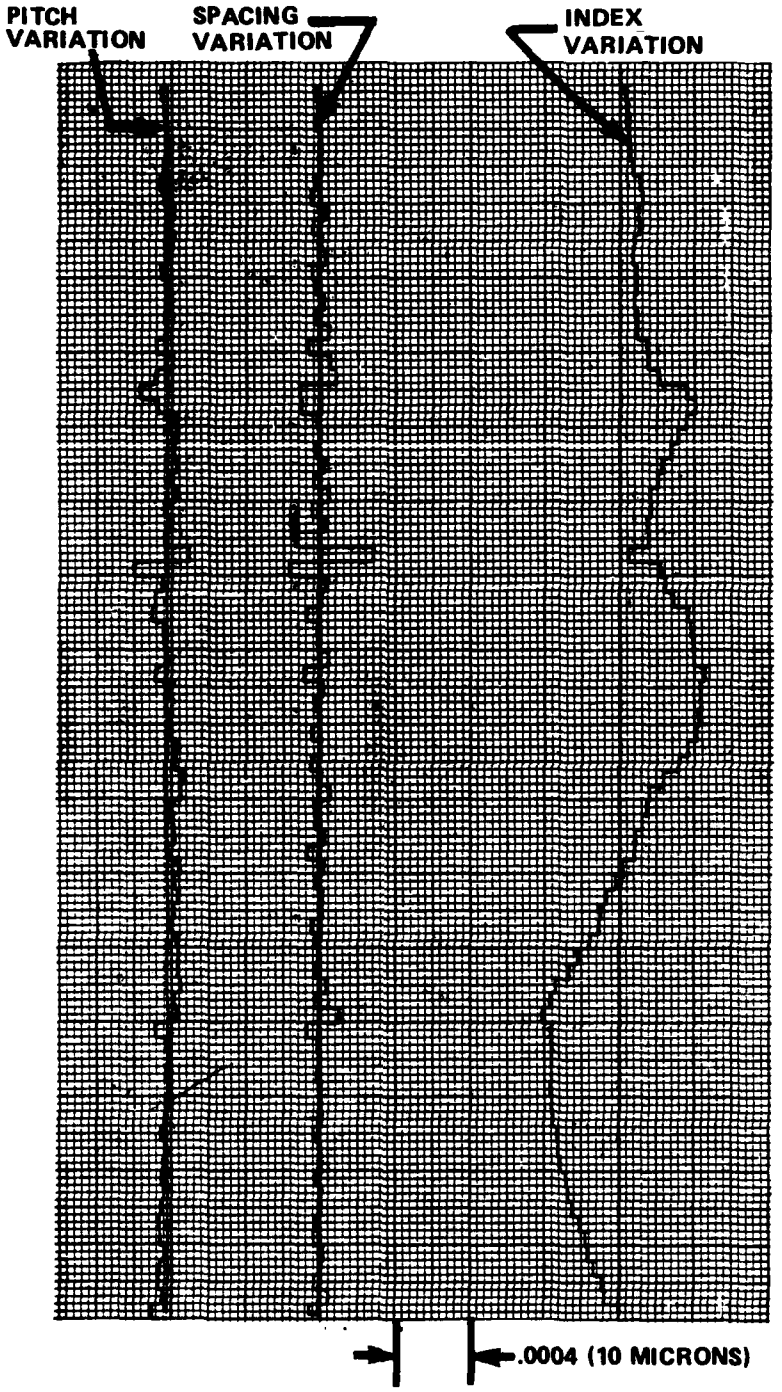

Figure 58. HCR Planet Gear Pitch, Spacing and Index (Drive Side/Ring Gear Mesh).

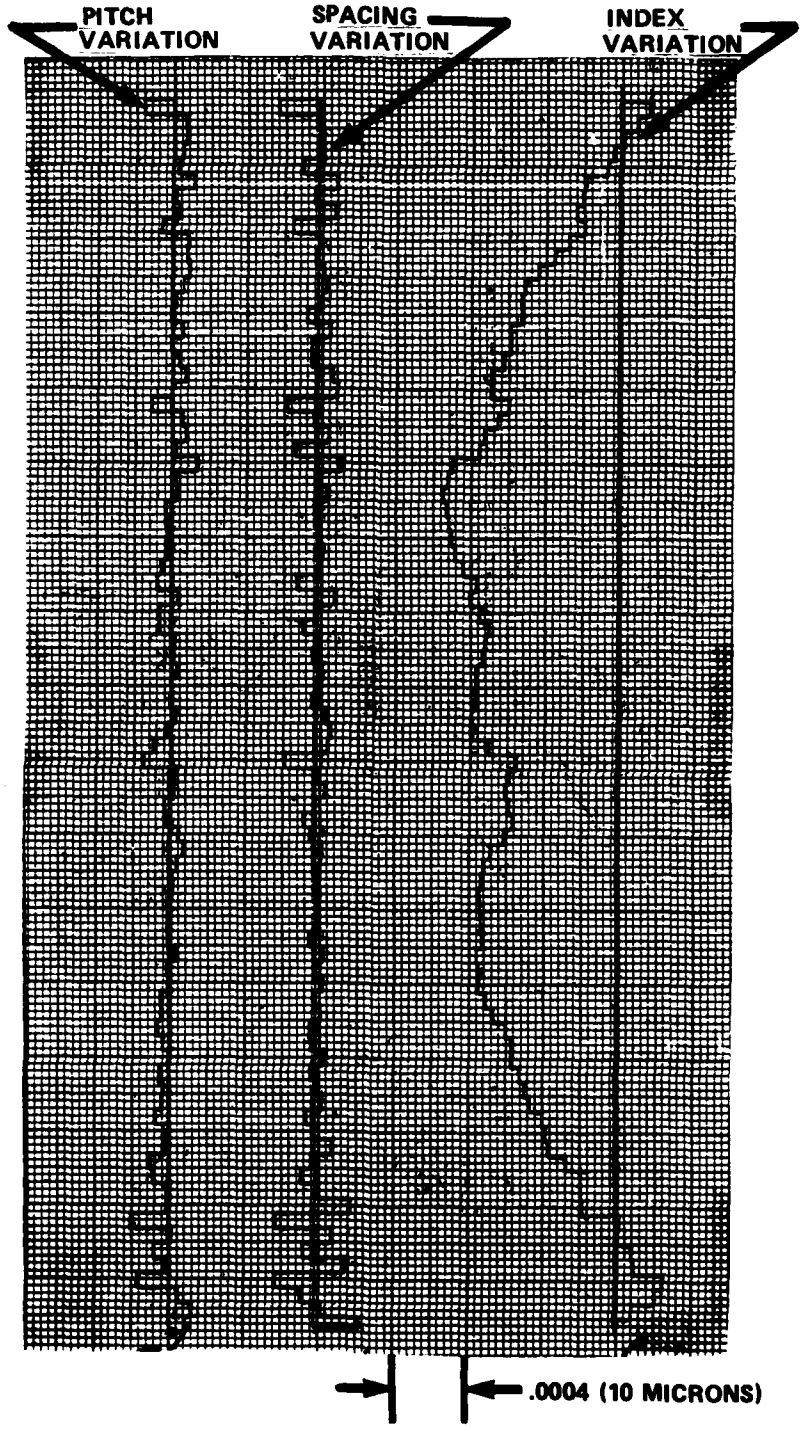

Figure 59. HCR Planet Gear Pitch, Spacing and Index (Coast Side/Sun Gear Mesh).

Table 8. BASELINE PLANETARY TOOTH MEASUREMENTS

Gear	Total Lead Error (in.)	Profile Tip (in.)	Profile True Involute Form (in.)	Pitch Variation (in.)	Spacing Variation (in.)
Sun	B/P*	B/P*	B/P*	B/P*	<.0002*
Planet #1 (Sun)	↓	↓	↓	↓	<.0002
#2 (Sun)					<.0002
#3 (Sun)					<.0002
#4 (Sun)					<.0002
#5 (Sun)					<.0002
#1 (Ring)					<.0002
#2 (Ring)					<.0002
#3 (Ring)					<.0002
#4 (Ring)					<.0002
#5 (Ring)					<.0002
Ring	B/P	B/P	B/P	B/P	<.0002
Sun	.0005 LH	-.0008	+.0003	+.00022	+.00022
Planet #1 (Sun)	.0002 RH	-.0010	.0000	+.00018	-.00027
#2 (Sun)	.0006 RH	-.0007	-.0001	+.00008	-.00010
#3 (Sun)	.0004 RH	-.0010	.0000	-.00018	+.00020
#4 (Sun)	.0003 RH	-.0008	.0000	+.00020	-.00020
#5 (Sun)	.0005 RH	-.0012	+.0002	+.00008	+.00008
#1 (Ring)	.0002 RH	-.0008	-.0001	+.00020	+.00022
#2 (Ring)	.0007 RH	-.0012	.0000	+.00012	-.00014
#3 (Ring)	.0001 RH	-.0010	.0000	+.00036	+.00052
#4 (Ring)	.0004 RH	-.0009	.0000	+.00016	+.00020
#5 (Ring)	.0002 RH	-.0012	+.0001	+.00010	+.00010
Ring	.0004 LH	-.0008	+.0002	+.00068	+.00064

*The baseline planetary was not reinspected after testing, but vendor inspection records confirm that all gear tooth dimensions are within blueprint (B/P) tolerance.

SUMMARY

Based on the ring gear accelerometer, the primary planet mesh frequency vibration levels are higher for the HCR gearset than for the baseline gearset. At twice planetary mesh frequency, HCR levels are comparable to or slightly lower. The change in vibratory level with horsepower appears to be more on the order of 3dB per doubling of horsepower rather than the 6dB expected value quoted in Reference 5. This 3dB trend is consistent in both the magnesium and stainless steel housings. The trends with horsepower and speed are similar and much smoother than described in Reference 6.

The difference in vibratory power levels between the baseline and HCR gearsets is probably caused by a combination of several factors. The most important of these is that the HCR gearset was initially designed and built to fully use the benefits of HCR from a gear design, stress, and weight standpoint. Thus, for similar stress levels, the gear weight could be substantially reduced. However, vibration amplitudes are related to the volume of stressed material; the HCR gears had longer teeth and apparently larger deflections.

Another factor to be considered is the effect of tooth variations on the HCR gearset. Figure 54 shows that two ring gear teeth are out of tolerance by a factor of 2 to 3 and one planet gear tooth had an out-of-tolerance condition of about twice that of the blueprint value (Table 3). This spacing variation would increase all sidebands around the mesh frequency (References 7 and 8). This effect is reflected in Figure 44. The tolerances used for the HCR gearset were the same as those used for the baseline gearset. Closer tolerances may be required for HCR gears to achieve lower vibration levels. It should be noted that if these sidebands were reduced, the overall power content in the bandwidth around the gear mesh frequency of the HCR planetary would be lower than the baseline planetary, since the planetary mesh harmonics are lower.

---

5. Mitchell, L.D.; Gear Noise: The Purchaser's and the Manufacturer's View. Proceedings of Purdue Noise Control Engineering, pp 95-106, 1971.
6. Marze, H.J., and d'Ambra, F.; Helicopter Internal Noise Reduction Research and Development: Application to the SA360 and SA365 Dauphin. Proceedings on International Specialists Symposium, NASA-Langley Research Center, Hampton VA, May 22-24, 1978.

A variety of reasons can be given for the presence of vibratory energy at gear mesh frequency, its harmonics, and sidebands at planet carrier speed around these harmonics. Adjacent gear tooth pitch variation causes multiple harmonics of once-per-revolution except for tooth mesh frequency. Involute profile variation increases gear mesh excitation and its harmonics. Eccentricity or gear pitch line runout produces once-per-rev gear mesh excitation and its harmonics modulated at plus or minus all harmonics of carrier rotation (References 7 and 8).

While high contact ratios are theoretically better for noise and vibration, it may be that variations in contact ratio are even more important than the actual contact ratio. For both HCR and standard designs, special attention to profile modification (tip relief) is necessary to account for tooth deflections. Additional factors which improve vibration levels are lower pressure angles and finer pitch. Lower speeds and lower tooth loads are also beneficial from a vibration and noise viewpoint. The vibration levels are generally accepted (Reference 5) to be related by

$$\text{Noise } \alpha \text{ 20 log } \frac{V}{V_o} \tag{14}$$

$$\text{Noise } \alpha \text{ 20 log } \frac{L}{L_o} \tag{15}$$

$$\text{Noise } \alpha \text{ 20 log } \frac{P}{P_o} \tag{16}$$

where V is speed, L is tooth load, P is power, and the subscripts indicate reference level. These relationships reflect that doubling the speed, load or power increases vibration and noise level by about 6dB.

The stainless steel housing had higher vibratory levels than the baseline magnesium housing (Figures 31 through 36), which was an expected result. The lighter stainless steel housing has more resonances as calculated with NASTRAN and shown in Figure 60. Higher vibratory response levels for the same energy flow result because of the lower mass of the structure as well as the lower damping level inherent in stainless steel.

---

7. Welbourn, D.B.; Fundamental Knowledge of Gear Noise - A Survey. The Institute of Mechanical Engineers, London, C117/79, July 1979.
8. Welbourn, D.B.; Gear Noise Spectra - A Rational Explanation. ASME 77-DET-38, 1977.

The change in vibratory level with speed is approximately 5dB over the speed range tested. The expected value would be on the order of 1-2dB since the variation is 20 log (V/V_O). Some variation may be caused by variations in contact ratio and load distribution with speed. Future analysis of this data using techniques contained in References 9 and 10 may clarify the explanations for these differences.

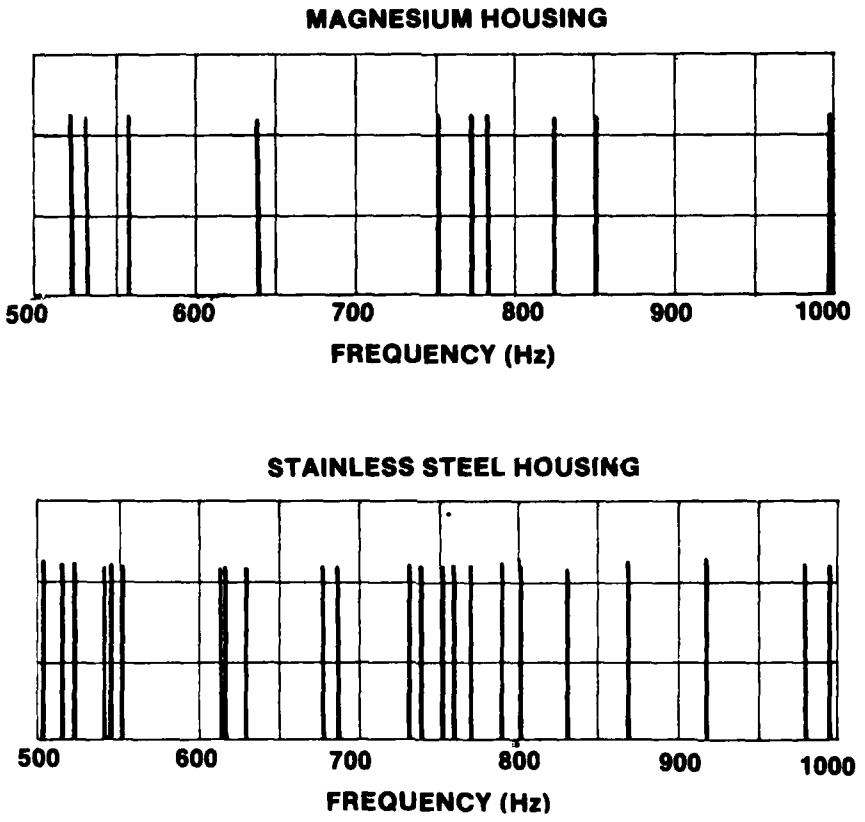

Figure 60. NASTRAN Calculated Natural Frequencies.

---

9. Mark, W.D.; Analysis of the Vibratory Excitation of Gear Systems: Basic Theory, JASA 63(5), May 1978, pp. 1409-1430.
10. Mark, W.D.; Analysis of the Vibratory Excitation of Gear Systems: Tooth Error Representatives, Approximations, and Application, JASA 66(6), December 1979, pp. 1758-1787.

CONCLUSIONS

Tests conducted under this program were limited in scope, in that only one high contact ratio gearset and one experimental housing were tested; results may have been peculiar to the test hardware. Based on the results of this effort, it is concluded that:

1 The high contact ratio (HCR) buttress planetary had slightly higher acoustic/vibration levels than the baseline (standard contact ratio) planetary gearset.

2. The higher vibration levels probably resulted because the HCR planetary face widths were approximately 15% less than the baseline planetary, producing approximately the same stress levels in each design.

3. The vibration levels of the HCR planetary were comparable to or lower than the baseline planetary at harmonics above the planetary mesh frequncy.

4. The vibration at the planetary mesh frequency was higher for the HCR planetary than the baseline planetary; this was true with both the magnesium and the stainless steel housing at all accelerometer locations for all power and speed conditions.

5. The HCR planetary had higher levels of sideband vibration than the baseline planetary.

6. Vibration levels at the planetary mesh frequency for the stainless steel housing with the HCR planetary were not directly proportional to applied load and generally leveled off after reaching approximately half of rated power.

7. The stainless steel housing had significantly higher vibration levels than the magnesium housing for the same loading conditions and with both planetary gearsets.

8. The increased vibration with the stainless steel housing is probably associated with the thin housing walls resulting in a greater modal density and larger vibration levels (because of lower mass and lower damping).

9. There continues to be a critical need for demonstrating the effects of transmission component concepts which attempt to simultaneously reduce system weight (gearbox and cabin noise treatment weight), increase reliability, and reduce noise.

RECOMMENDATIONS

1. Additional design and testing to evaluate helicopter transmission experimental high contact ratio planetary gearsets is recommended to:

   a. Positively identify the impact of changes in tooth spacing and profile variation and in contact ratio (the proper range for quieter gears).

   b. Identify the sensitivity of vibration to gear tooth stress, load sharing, and general mesh smoothness.

   c. Determine and correlate with design procedures the acceptable limits of sensitive parameters such as gear tooth manufacturing variations, proper contact ratio range, required gear rim backup material, and preferred pressure angles.

2. Additional design and testing to evaluate helicopter transmission experimental housings is recommended to:

   a. Investigate stainless steel housing designs which provide reinforcement in the form of corrugated sheet (or equivalent method) instead of external structural ribs to provide increased stiffness and damping for the housing walls.

   b. Evaluate fabricated housing designs for potential acoustic impact by testing simple shapes (such as a plate or shell) to identify wall configurations with minimum vibration.

3. A test facility evaluation of a series of production gearboxes is recommended, to more accurately determine the effects of gearbox acoustic vibration on helicopter cabin noise levels, to be followed by an evaluation of these gearboxes installed in helicopters.

END

FILMED

11-85

DTIC